Qualification of innovative floating substructures for 10MW wind turbines and water depths greater than 50m

Project acronym	LIFES50+
Grant agreement	640741
	Collaborative project
Start date	2015-06-01
Duration	40 months

Deliverable D7.8 Required numerical model fidelity in various design phases

Lead Beneficiary	DTU
Due date	2018-05-31
Delivery date	2018-07-04
Dissemination level	Public
Status	Final
Classification	Unrestricted
Keywords	Numerical models, state-of-the-art, floating wind turbines
Company document number	Click here to enter text.

The research leading to these results has received funding from the European Union Horizon2020 programme under the agreement H2020-LCE-2014-1-640741.

Disclaimer

The content of the publication herein is the sole responsibility of the publishers and it does not necessarily represent the views expressed by the European Commission or its services.

While the information contained in the documents is believed to be accurate, the authors(s) or any other participant in the LIFES50+ consortium make no warranty of any kind with regard to this material including, but not limited to the implied warranties of merchantability and fitness for a particular purpose.

Neither the LIFES50+ Consortium nor any of its members, their officers, employees or agents shall be responsible or liable in negligence or otherwise howsoever in respect of any inaccuracy or omission herein.

Without derogating from the generality of the foregoing neither the LIFES50+ Consortium nor any of its members, their officers, employees or agents shall be liable for any direct or indirect or consequential loss or damage caused by or arising from any information advice or inaccuracy or omission herein.

Document information

Version	Date	Description	
1	2018-06-13	Version 1	
		Prepared by	Madsen, F.J.; Pegalajar-Jurado, A.; Bredmose, H.; Borg, M.; Müller. K.
		Reviewed by	H. Bredmose
		Approved by	H. Bredmose
2	2018-06-21	Draft	
		Prepared by	Madsen, F.J.; Pegalajar-Jurado, A.; Bredmose, H.; Borg, M.; Müller. K.; Matha, D.
		Reviewed by	D. Matha; Andreas Manjock
		Approved by	H. Bredmose
3	2018-07-02	Final	
		Prepared by	Madsen, F.J.; Pegalajar-Jurado, A.; Bredmose, H.; Borg, M.; Müller. K.; Matha, D.
		Reviewed by	H. Bredmose
		Approved by	H. Bredmose
4	2018-07-03	Final version for QA before submission	
		Prepared by	Bredmose
		Reviewed by	Jan Arthur Norbeck
		Approved by	Petter Andreas Berthelsen

Authors	Organization
Madsen, F.J.	DTU
Pegalajar-Jurado, A.	DTU
Bredmose, H.	DTU
Borg, M.	DTU
Müller, K.	USTUTT
Matha, D.	RAMBOLL

Contributors Organization

Definitions & Abbreviations

AP	Anchor point
CM	Centre of mass
COD	Co-directional
CP	Connection point
DLB	Design load basis
DLC	Design Load Case
DoF	Degree of freedom
ECM	Extreme current model
ESS	Extreme sea state
ETM	Extreme turbulence model
EWLR	Extreme water level range
EWM	Extreme wind speed model
F	Fatigue
FAST	Fatigue, Aerodynamics, Structures and Turbulence
FLP	Fairlead point
FLS	Fatigue limit state
FOWT	Floating offshore wind turbine
MIS	Misaligned
MUL	Multi-directional
MWL	Mean water level
N	Normal
NCM	Normal current model
NREL	National Renewable Energy Laboratory
NSS	Normal sea state
NTM	Normal turbulence model
PSD	Power spectral density
QuLAF	Quick Load Analysis of Floating wind turbines
RWT	Reference Wind Turbine
SSS	Severe sea state
SWL	Still water level
U	Ultimate strength
ULS	Ultimate limit state
UNI	Uni-directional
WP	Work Package
WSP	Wind speed

Executive Summary

The design of floaters for offshore wind turbines usually follows three steps: Conceptual design, basic design, and detailed design. Within basic design, state-of-the-art models such as FAST, Bladed and HAWC2 are used to calculate time domain loads under various design load cases. Faster models, however, may be valuable in the conceptual design phase, where fast answers for response levels and load levels may affect the design at an early stage. Such models also enables the use of optimization methods in the design.

The purpose of the present deliverable is to answer two questions, namely

- How accurate results can you obtain from simplified models for different load cases?
- In what load cases is it sufficient to apply the simplified models?

Based on a selected subset of critical load cases, this is investigated through comparison of the simplified model QuLAF and the state-of-the-art model FAST for the OO-Star Wind Floater Semi 10MW floater-turbine configuration of LIFES50+. A review of simulation requirements and critical environmental conditions is provided.

Next, the two models are presented and the limitations of QuLAF based on previous results are discussed. The limitations are (A) an under-prediction of the wave excitation force at large sea states due to the omission of viscous drag forcing; (B) an under-prediction of the wind-induced response around rated wind speed, where the controller in the full FAST model switches between the partial-load and full-load regimes; (C) an over-predicted aerodynamic damping for the tower mode motion which leads to under-prediction of the nacelle acceleration and (D) the restriction to planar motion.

A comparative simulation study based on the planar version of DLC 1.2, 1.3, 1.6, 2.1 and 6.1 is next presented. The FLS (fatigue) analysis shows that the simplified model is very good at estimating the damage-equivalent bending moment at the tower base but has problems with the nacelle acceleration. The high under-prediction in the nacelle acceleration is likely due to an over-prediction of the aerodynamic damping of the nacelle motion.
The same picture of the nacelle acceleration being too under-predicted in the simplified model is also present in the ULS analysis. The largest tower base bending moments are generally over-predicted. It is observed though, that while stronger wind leads to an over-prediction, stronger waves leads to an under-prediction. Thus, in DLC 1.6 where the largest load was obtained at 10.3 m/s a perfect match between the two models is found.
Regarding the platform motions, the largest surge responses are achieved in DLC1.3 and DLC1.6 with a 3% over-prediction and 11% under-prediction, respectively. The largest heave motions are generally very well matched by the two models and achieves highest values in the ESS (Extreme Sea State) cases. Lastly the ultimate pitch responses are obtained in DLC1.3 and DLC1.6 both at rated conditions and within 4% deviation.

Despite the discussed limitations, QuLAF is found to be a quite accurate load and response prediction tool for aligned wind-wave load cases, especially for tower bending moments, heave and pitch motions. Although a full design load basis evaluation with a state-of-the-art model must be carried out for the final design, the present results shows the potential of QuLAF model application in the preliminary design phase to predict loads at an early stage, explore design variations and enable optimization within floater design for offshore wind turbines.

Contents

1 Introduction 7
1.1 Advanced models overview 7
1.2 Structure of the present deliverable 8
2 Simulation requirements – summary of D7.7 9
2.1 Design driving load cases 9
2.2 Relevant environmental conditions 9
2.3 Simulation requirements 11
3 Definition of present study 12
4 State-of-the-art model of the OO-Star Wind Floater Semi 10MW 13
4.1 Wind turbine and controller 14
4.2 The floater and modelling of the tower 14
4.3 Approach for hydrodynamic modelling 15
4.4 Mooring system 16
4.5 Approach to varying equilibrium position over load cases 16
5 The simplified model: QuLAF 17
5.1 Overall model philosophy 17
5.2 Parent model 17
5.3 Planar degrees of freedom 17
5.4 Linearized equations of motion 18
5.5 Hydrodynamic viscous forcing and viscous damping 19
5.6 Pre-computed aerodynamic forcing and damping 20
5.7 Frequency domain motion solver 20
5.8 Static offset 21
5.9 Summary of model limitations 21
5.10 Summary: What is needed to run the model 21
6 Results 23
6.1 FLS simulation study 23
6.2 ULS simulation study 25
7 Design Practice of Floating Wind Turbines 39
8 Conclusion and recommended practices 42
9 References 44

1 Introduction

The present deliverable concerns the applicability of simplified models in the design of floaters for offshore wind turbines in the 10MW class. The work is based on WP4, where both a state-of-the-art model and a simplified model have been developed.

The idea of work package 4 is to apply tools at varying fidelity during the different design phases. In pre-design, where fast answers are needed, the accuracy requirements may be relaxed and allow for application of low-dimensional models. This may even enable the application of optimization methods and is an improvement over experience based or static conceptual design methods in early stages. Next, when the concept design is more converged, state-of-the art models like FAST, HAWC2 and Bladed are used in the design validation; and eventually more advanced models can be used for detailed design tasks. For certification, loads analysis of the full set of design load cases according to recognized standards using state-of-the-art models is required. This is illustrated in the schematic in Figure 1 where model accuracy is depicted against CPU execution time.

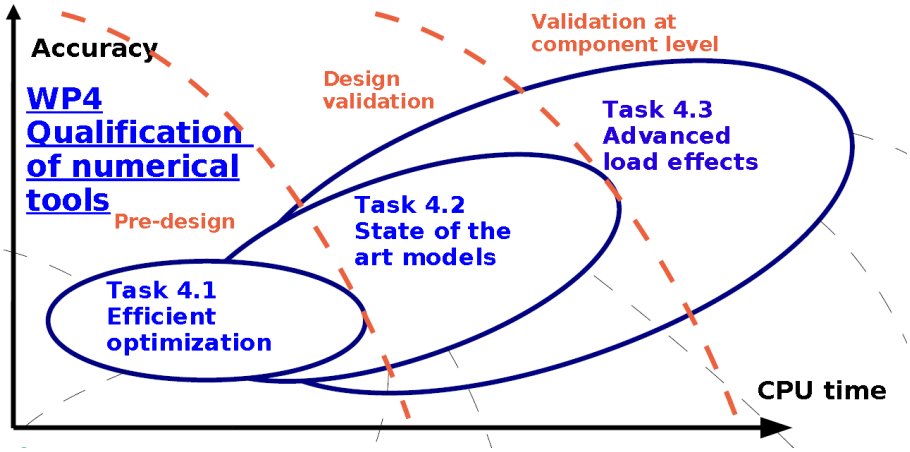

Figure 1: CPU-time versus accuracy for design models. Task division in LIFES50+ WP4.

The scope of the present deliverable is to answer two questions, namely

- How accurate results can you obtain from simplified models for different load cases?
- In what load cases is it sufficient to apply the simplified models?

To this end a FAST state-of-the-art model [1] is applied to the OO Star 10MW Semi concept for a number of design load cases (DLCs) and the results are compared to computations with the simplified QuLAF model [2]. The FAST model has been presented in [1] and in [3] D4.5 *State-of-the-art models for the two public 10MW floater concepts*, while an early version of the QuLAF model was presented in [4]. A brief description of both models are provided in section 4 and 5.

1.1 Advanced models overview

While the mapping of accuracy between the simplified models and the state-of-the-art models is the subject of the present work, the similar comparison of advanced models and state-of-the-art models will be described in later deliverables in WP4. Nevertheless, a brief overview of the five model developments at the advanced level is given below More detail can be found in D4.7 *Models for advanced load effects and loads at component level* [5].

Inclusion of elasticity in dynamic substructure response calculations

Motivated by the need for material saving and substantial size of the 10MW class floaters for offshore wind turbines, a method for inclusion of elasticity in dynamic substructure response calculations is developed. This enables a more accurate determination of the natural frequencies for the full floater-turbine configuration and provides a method for calculation of the internal stresses in the floater structure. The framework is implemented in the HAWC2 aero-elastic model of DTU and utilizes the generalized mode feature in WAMIT. An example of application to the INNWIND.EU TripleSpar floater is presented in D4.7.

Nonlinear wave forcing

The forcing from nonlinear waves leads to response at the floater natural frequencies from sub-harmonic waves and may also excite tower vibrations by super-harmonic forcing. Two methods are wide-spread for the prediction of these effects namely a) the second-order panel approach where Quadratic Transfer Functions (QTF's) for wave forcing are pre-computed and next used in the response calculations; and b) higher-order wave kinematics in combination with the slender-body Morison force model (strip theory). In D4.7, the QTF approach is outlined. Next a slender-body study in FAST with nonlinear kinematics from a fully nonlinear wave model, second-order kinematics and linear kinematics is presented with inter-comparison to model tests for a TLP turbine configuration from DTU and DHI.

Validation of OpenFOAM CFD solver for added mass and damping

An OpenFOAM hydrodynamic CFD (Computational Fluid Dynamics) model is setup for the LIFES50+ OO-Star Wind Floater Semi 10MW. The solver is a 6 degree of freedom solver with free surface and is validated with respect to added mass and damping properties by comparison to results of WAMIT. The perspective of the solver is to allow coupled computations with an outer wave model that drives the boundary conditions to a localized CFD domain. In D4.7, the validation part against WAMIT data and decay tests in FAST are presented.

Fluid-Multibody coupled solver for high-fidelity hydrodynamic analysis

A second CFD solver with a coupling of Simpack and CFX has been developed. Details on the coupling technique to rotor load calculations are given and the approach to wave generation is detailed in D4.7. Next, an example of application to the IDEOL floater in regular waves is provided.

Vortex-based aerodynamic load calculations

A vortex-based aerodynamic rotor model is presented as an alternative to the classical Blade Element Momentum (BEM) approach. Vortex methods represent a level of modelling between BEM and CFD. The present method is coupled through SIMPACK to include also floater surge and pitch motion. Next results of the model are compared to BEM calculations for generic step-motion and sinusoidal motion.

1.2 Structure of the present deliverable

The purpose of the present deliverable is to assess the accuracy of the simplified model by comparison to the state-of-the-art model for several design load cases. To put the selection of load cases into context, a summary of D7.7 [6] with respect to simulation requirements is provided in section 2. Next, section 3 details the scope of the present study with respect to the chosen design load cases and the chosen analysis of the results. The FAST state-of-the-art model and the QuLAF simplified model are outlined in sections 4 and 5. The results are presented in Section 6 and linked into the design practice for floating wind

turbines in Section 7. The report concludes with a presentation of recommended practice in terms of a summary of the findings in Section 8.

2 Simulation requirements – summary of D7.7

Extensive work was carried out in D7.7 on 'Identification of critical environmental conditions and design load cases' [6]. The main findings are summarised here. The work aimed to answer the following questions within LIFES50+ and to provide methods to their answer for other sites and turbine configurations:

1. Can a subset of load cases from the Design basis be identified that may be design driving across all substructure concepts?
2. Within these most relevant load cases,
    a. What are the most relevant environmental conditions?
    b. What are requirements for the setup of the simulations?

The findings are summarized in the following.

2.1 Design driving load cases

While a complete set of standard load cases, including the defined combinations of environmental and operational parameters must be performed to achieve the required accuracy for the final development stages of FOWT, it may support the overall speed of the design process to focus on a subset of critical design load cases in an earlier design stage. While this subset will be very specific to a considered system (including controller, wind turbine, substructure concept and station keeping system), the aim of this work was to present a set of load cases that can generally be considered of interest for all FOWT systems.

The selected load cases comprise fatigue load cases during normal operation between cut-in and cut-out wind speed (DLC1.2) and two extreme load cases. The extreme situation of power production during a severe sea state (DLC1.6) and idling during a 50-year storm event (DLC6.1) generally produce critical loads for the rotor-nacelle assembly, the tower, the floater and the station keeping system. It is noted that due to the conservative setup of DLC1.6 in the LIFES50+ design basis (applying a 1- and 50year significant wave height across the wind regime), this load case may be less relevant, when more detailed data of the environment is available.

In D7.8, due to the simplified aerodynamic modelling applied in many simplified numerical models, two load cases were added in this work that may be of challenge. This is (1) DLC1.3, which assumes a more conservative turbulence regime, resulting in more pronounced aerodynamic loading and (2) DLC 2.1 with a grid loss, which implements some challenge towards an optimal controller response. This response is highly sensitive to the wind environment as well and hence it is also considered as particular challenging for the modelling capacities of simplified models.

2.2 Relevant environmental conditions

Further to the identification of design driving load cases, the most relevant environmental parameters within the load cases were identified. This was done through a global sensitivity analysis (GSA) based on analysis of variance (ANOVA) performed within the different load cases. Figure 2.1 shows exemplarily the results of a simulation study which was performed to investigate the different impact of wind

speed, wave height and wave period on the FOWT system. Next to providing a large-scale robustness check of the numerical model and the design, GSA helped to quantify the impact of different environmental conditions on different system components. This was done using chi-squared testing, which provides a p-value indicating the likelihood of independence towards a given environmental variable (i.e. a smaller p-value indicates a strong influence on the loading). The results of the GSA measures were summarized in ranking tables, one of which is shown in Table 2-1. Relevant results for the concepts and site under consideration where (generalized for all three considered load cases):

- Wind speed, wave height and wave period of major importance
- Directionality of wind and waves also of high influence, when combined to wind-wave-misalignment. The most severe cases are related to the substructure geometry
- Impact of wind speed and wave period is not monotonic, hence special care is to be taken if a binning or reduction of these environments is applied.
- Some interaction of wave periods and wind turbine dynamic behaviour is likely to be of importance for highest loading from wave periods.
- Current speed and current directionality as well as water depth was found of minor significance, although this may change with increased variation of these variables.
- Variation of peak enhancement factor is of minor influence
- The influence of marine growth on mooring lines may influence the loading significantly, but the origin of influence is concept specific.

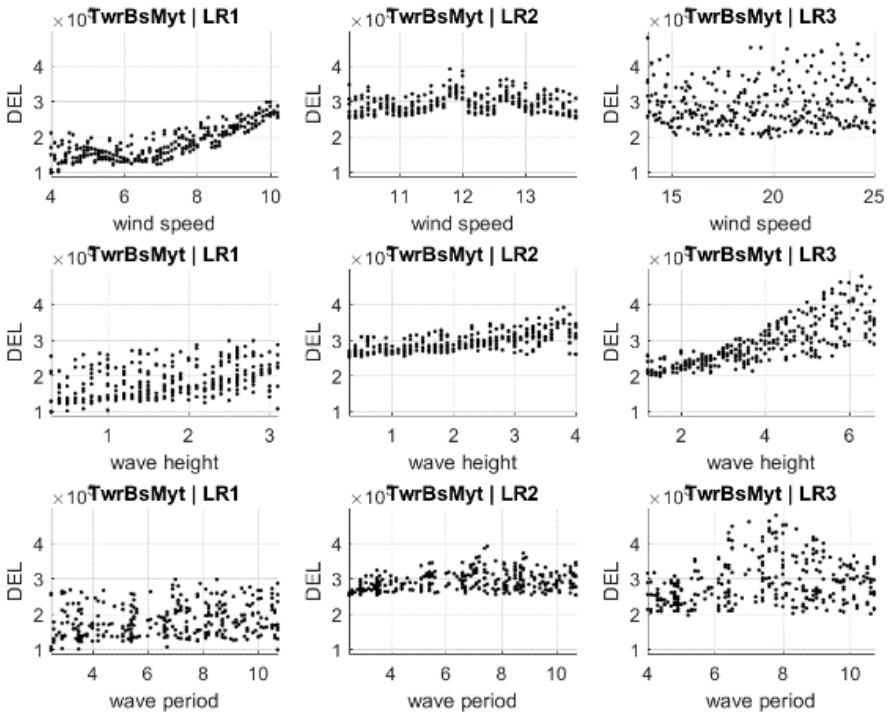

Figure 2.1: *LIFES50+ OO-Star Wind Floater Semi 10MW* Tower base fore-aft bending moment scatterplots of sensitivity analysis simulations considering variation of wind speed, wave height and wave period for three different load ranges (LR1: below rated, LR2: around rated, LR3: above rated) [6].

Table 2-1: Ranking table for most influential environmental parameters across different load ranges for Olav Olsen semi-submersible and DLC 1.2 considering wind speed, wave height and wave period.

rank	*region*	*p-value*
Blade root flapwise		
1	LR1 / wind speed	1.70E-51
2	LR3 / wind speed	9.64E-51
3	LR2 / wind speed	7.82E-44
4	LR2 / wave period	3.31E-01
5	LR3 / wave height	4.44E-01
6	LR1 / wave period	6.57E-01
7	LR1 / wave height	7.06E-01
8	LR2 / wave height	7.45E-01
9	LR3 / wave period	7.51E-01
Tower base fore-aft		
1	LR3 / wave height	8.58E-36
2	LR1 / wind speed	1.61E-30
3	LR2 / wave height	9.94E-19
4	LR2 / wind speed	8.58E-09
5	LR1 / wave height	1.49E-05
6	LR3 / wave period	3.24E-04
7	LR2 / wave period	1.12E-02
8	LR1 / wave period	3.42E-01
9	LR3 / wind speed	7.73E-01
Fairlead 1 tension		
1	LR3 / wave height	1.42E-43
2	LR2 / wave height	2.10E-41
3	LR1 / wave height	1.57E-18
4	LR1 / wind speed	3.34E-12
5	LR3 / wave period	1.68E-02
6	LR1 / wave period	8.68E-02
7	LR2 / wave period	3.62E-01
8	LR2 / wind speed	5.34E-01
9	LR3 / wind speed	7.78E-01

2.3 Simulation requirements

As guidelines are not providing quantitative values with respect to the simulation settings, methodologies were developed to aid the designer in ensuring converged solutions as well as quantifying the remaining uncertainty based on limited simulation length and seed number. For this, the following is proposed:

- Use *moving average* analysis in the assessment of proper initial conditions (without stochastic environment)
- Use *backwards standard deviation* analysis to ensure the negligence of initial transients in the load simulations (with stochastic environment).
- Use *bootstrapping* to assess uncertainty remaining due to considering a limited number of seeds. This may be of special relevance as the uncertainty is concept specific.

Additionally, a comparative study was performed to identify the trade-off between using longer simulation times compared to longer seed numbers (assuming a constant overall simulation time). Here, it was found that lower uncertainty / more conservatism in the results is to be expected if the statistical information is increased (e.g. if periodic wind seeds are applied, a longer simulation time may not lead

to overall increased statistical information. Then, using more seeds of shorter simulations may be beneficial). If the statistical content stays the same, and for the considered setup, no significant difference between choosing many short simulations or few long ones is expected.

3 Definition of present study

As described in [6] load cases are an inherent part in the wind turbine standards and define the specific design load criteria for the structural design according to defined classes of environmental conditions. These generic conditions describe wind, waves, gusts, currents, etc. and their related meteorological parameters in different classes of severity. The goal of conducting load cases is to cover all relevant load situations within the designated life time of the structure, but more importantly to cover all potential design-driving situations, i.e. the situations leading to critical design loading. The load cases consist of normal operation, extreme events, stand-still conditions and transient events such as start-up, shut-down, and fault conditions.

One could imagine that considering a full design load basis (DLB) setup consisting of all design load cases for a FOWT design could easily reach 10^4 different DLC's per concept. This can be computationally expensive, especially if they are carried out with time-domain numerical tools simulating at real-time CPU speed for several concepts. The advantage of faster tools is that they allow optimization in the initial design stage, where several designs are being explored with many design variables, thus has to be thoroughly examined and a broad overview of the system response and loads is desirable. The present study presents the mapping of accuracy between the simplified model QuLAF and the state-of-the-art model FAST.

Following the work of [6], where three critical design-driven load cases were derived and applied to the two concepts of LIFES50+; the OO-Star Wind Floater Semi 10MW and the NAUTILUS-10 floating structure. The selected load cases included fatigue during normal operation (DLC1.2), ultimate loads during power production in severe sea states (DLC1.6) and ultimate loads when the turbine is parked during a 50-year storm event (DLC6.1). However, for the present study of analysing the applicability of the simplified model QuLAF in the design phase of FOWT, it was decided to add two additional design load cases, namely ultimate loads during power production in extreme turbulence (DLC1.3) and ultimate loads during a transient event triggered by a loss of electrical network connection (DLC2.1). DLC1.3 was considered in order to fully evaluate the results of QuLAF by comparing with the baseline load case (DLC1.2) and the extreme sea state load case (DLC1.6). DLC2.1 was included in the study in order to see how well QuLAF would handle a transient event.

Table 2 shows the selection of load cases investigated in the present study. However, simplifications have been made to each load case since QuLAF only solves a 2D problem and is thus restricted to aligned wind and wave load situations. This also means that only in-plane loads, and motions has been investigated.

All normal sea states (NSS) load cases were based on the long term joint probability distribution of metocean parameters presented in [16], which were to be considered for the fatigue analysis. Ideally, one would use the site-specific data for the other DLCs with NSS, but in order to have DLC1.2 to also serve as a baseline load case for the ULS DLCs it was decided to use the joint probability distribution NSS. This also means that each wind speed in each load case had three realisations of the peak period.

Six different wind and wave seeds were simulated for each environmental condition, with the only exception of DLC2.1 where four seeds were deemed sufficient, as the maximum loads in this case are governed by the transient event. For each of each environmental condition the characteristic value is the mean of the maximum values of the different realizations (seeds) and is used for evaluation.

Furthermore, a simulation time of 5400s with the same length of turbulent wind field was used for all the load cases including 1800s run-in-time to remove any transient response in the time-domain model. This run-in-time corresponds to approximately 9 surge periods, which was deemed acceptable for the lowest sea state, where the sub-harmonic influence is highest. It should also be noted that initial conditions were applied to each load case situation based on the results from the static equilibrium case and the step wind case in [3].

Table 2: Selection of design load cases. Note that the comparative study was limited to aligned wind-wave conditions only, due to the restriction of QuLAF to planar motion.

Load case	*Description*	*Wind conditions*		*Marine conditions*			*Wind and waves directionality*	*Type of analysis*	*PSF*
		WSP	*Turb.*	*Waves*	*Sea currents*	*Water level*			
DLC1.2	Power production during normal operation	$V_{in} < V_{hub} < V_{out}$	NTM	NSS Joint prob. Distribution of H_s, T_p, V_{hub}	No currents	NWLR or ≥MSL	MIS, MUL	F/U	*/N
DLC1.3	Power production during extreme turbulence	$V_{in} < V_{hub} < V_{out}$	ETM	NSS $H_s = E[H_s\|V_{hub}]$	NCM	MSL	COD, UNI	U	N
DLC1.6	Power production during severe sea states	$V_{in} < V_{hub} < V_{out}$	NTM	SSS $H_s = H_{s,SSS}$	NCM	NWLR	COD, UNI	U	N
DLC2.1	Power production with grid loss	$V_{in} < V_{hub} < V_{out}$	NTM	NSS $H_s = E[H_s\|V_{hub}]$	NCM	MSL	COD, UNI	U	N
DLC6.1	Parked in extreme wind	$V_{hub} = V_{ref,50y}$	EWM	ESS $H_s = H_{s,50y}$	ECM	EWLR	MIS, MUL	U	N

4 State-of-the-art model of the OO-Star Wind Floater Semi 10MW

The LIFES50+ OO-Star Wind Floater Semi 10MW, is extensively described in [7]. A FAST model of the DTU 10MW reference wind turbine at this floater has been made in the LIFES50+ and reported in [3], [1]. We here summarize the main specifications of the floating wind turbine configuration and the modelling approach in the FAST model. The information is extracted from [3]. We will refer to this FAST model as the 'state-of-the-art' model and define a simplified model in section 5.

4.1 Wind turbine and controller

The DTU 10MW Reference Wind Turbine (RWT) is described in [8] (see Figure 3). Further, the FAST implementation of the land-based configuration of the DTU 10MW RWT is described in [9]. To account for the freeboard of the floating substructure and to maintain the hub height at 119 m, the turbine tower was shortened for both floating substructures, as detailed in [7].

Figure 3: DTU 10MW RWT

In LIFES50+ the basic DTU Wind Energy controller is employed [10]. The DTU controller consists of two different controllers for the partial load region (i.e. operation below rated wind speed) and the full load region (i.e. operation above rated wind speed), and a mechanism that smoothly switches between these two controllers around rated wind speed. Details of the controller can be found in [10]. The pole-placement method [11] was used to tune the proportional-integral (PI) controllers where needed. The OO-Star Semi controller was tuned by Dr. techn. Olav Olsen AS.

4.2 The floater and modelling of the tower

The OO-Star Wind Floater Semi 10MW is a semi-sub floater made of post-tensioned concrete. Some of the main properties of the floater are collected in Table 3 below and a sketch of the full floater and turbine configuration is given in Figure 3.

Table 3: Main properties of the OO-Star Semi floating substructure

Type	Material	Draft	Freeboard	Displaced volume	Floating substruc-ture mass
		[m]	[m]	[m^3]	[kg]
Semisubmersible	Post-tensioned concrete	22.00	11.00	2.3509E+04	2.1709E+07

Figure 3: The OO-Star Semi floating substructure. Figure provided by Dr. techn. Olav Olsen AS

To capture some of the floating substructure flexibility, the portion of substructure between still water level (SWL) and tower interface has been modelled as part of the tower. This *semi-flexible* approach entails extending the definition of the tower to SWL and adding one more tower section to the tables of tower properties given in [7]. Further details on this approach and a discussion of the effects on the natural frequencies of the coupled floater-turbine system is given in [1].

4.3 Approach for hydrodynamic modelling

The hydrodynamic modelling is based on pre-computed linear radiation-diffraction coefficients, obtained by the frequency-domain, potential-flow solver WAMIT [12]. No second-order effects were included. The results are applied in the FAST model through the convolution approach resulting from the Cummins equation [13]. The hydrodynamic properties from WAMIT are the hydrostatic restoring matrix $\boldsymbol{C_{hst}}$, the hydrodynamic added mass matrix $\boldsymbol{A}(\omega)$ and radiation damping matrix $\boldsymbol{B}(\omega)$, and the vector of wave diffraction forces $\boldsymbol{X}(\omega)$. The reader should note that added mass, radiation damping, and wave diffraction forces depend on the angular frequency, ω, and that all properties are computed with respect to the point of flotation. These properties, together with the floating substructure inertia matrix $\boldsymbol{M}$, the Fourier coefficients for the floating substructure motion in 6 degrees of freedom (DoF) $\hat{\boldsymbol{\xi}}(\omega)$ and the Fourier coefficients of the incident wave surface elevation $\hat{\eta}(\omega)$, define the equation of motion for an unrestrained, floating body in the frequency domain:

$$\left[-\omega^2\left(\boldsymbol{M}+\boldsymbol{A}(\omega)\right)+i\omega\boldsymbol{B}(\omega)+\boldsymbol{C_{hst}}\right]\hat{\boldsymbol{\xi}}(\omega)=\boldsymbol{X}(\omega)\hat{\eta}(\omega) \qquad (1)$$

The equation is converted to the time domain through the convolution integral [13] and thus solved in the time domain within FAST. This allows for a full coupling to the rotor dynamics and mooring dynamics.

Viscous drag is not captured by potential-flow solvers. It is included by the drag term in the Morison equation, which provides the transversal drag force df_{drag} on a cylindrical member section of length dz:

$$df=\frac{1}{2}\rho C_D D v_{rel}|v_{rel}|dz \qquad (2)$$

Here ρ is the fluid density, C_D is an appropriate drag coefficient, D is the cylinder diameter, and v_{rel} is the relative velocity between the body and the fluid, projected to the normal of the cylinder axis. Analogously, the axial drag on a circular heave plate is computed as:

$$F = \frac{1}{2}\rho C_{DHP} A_{HP} v_{rel} |v_{rel}| \quad (3)$$

where C_{DHP} is a drag coefficient and A_{HP} is the heave plate area projected on the plane normal to the motion.

Since FAST allows only cylindrical members of the floater for the Morison description, special efforts were made to represent the effect of the heave plates in both surge/sway, heave and pitch/roll. This is detailed in [1].

4.4 Mooring system

The mooring line properties for the OO-Star Semi floating substructure are defined in [7]. Each mooring line consists of an upper line connecting the fairlead point (FLP) to a connection point (CP) with a clump mass of 50000 kg (effective mass in water). Next follows a lower line between the connection point and the anchor point (AP). The information is detailed in Table 4 below.

Table 4: Mooring lines for the OO-Star Semi floating substructure

Line #	Anchor coordinates			Connection coordinates			Fairlead coordinates		
	X	Y	Z	X	Y	Z	X	Y	Z
	[m]	[m]	[m]	[m]	[m]	[m]	[m]	[m]	[m]
1	-691	0	-130	-117.9	0	-81.1	-	-	-
2	345.5	598.42	-130	58.95	102.10	-81.1	-	-	-
3	345.5	-598.42	-130	58.95	-102.10	-81.1	-	-	-
4	-	-	-	-117.9	0	-81.1	-44	0	9.5
5	-	-	-	58.95	102.10	-81.1	22	38.11	9.5
6	-	-	-	58.95	-102.10	-81.1	22	-38.11	9.5

The mooring system was modelled with the MoorDyn module [14]. MoorDyn provides the option of multi-segmented lines and clump weights, necessary for the correct modelling of the OO-Star Semi mooring lines. MoorDyn captures dynamic effects from the line elasticity and inertia and hydrodynamic forces on the segments, but the hydrodynamic loads are applied to a mooring line moving in still water.

4.5 Approach to varying equilibrium position over load cases

Generally, a floating wind turbine will oscillate around different equilibrium positions for different environmental conditions. Especially the mean thrust at each wind speed leads to a mean offset of the floater and thus defines an equilibrium position for each simulation. Ideally, one would compute radiation-diffraction properties for each equilibrium position and use the corresponding WAMIT data for each environmental condition. For the FAST model, however, a simpler approach was followed, where hydrostatic and hydrodynamic properties for each floating substructure were computed for a single reference position, which corresponds to the floating structure in calm water and with no wind.

5 The simplified model: QuLAF

A simplified model of the floater-turbine configuration was implemented in terms of the QuLAF model (Quick Load Analysis- Floating). The modelling concept and philosophy is described in [15] for bottom-fixed substructures and in [2] for floating wind turbines, see also LIFES50+ D4.1 *Simple numerical models for upscaled design* [4]. The main concept and ideas of the model are summarized here.

5.1 Overall model philosophy

The purpose of QuLAF is to provide fast answers about design loads and natural frequencies already in the pre-design phase, where many design variations are tried before a concept design for the basic design is chosen. The simplicity and efficiency are obtained by inclusion of only few degrees of freedom, linearization of the equations of motion, pre-computation of aero-dynamic rotor forcing and damping; and solution of the equations of motion in the frequency domain. These elements are described briefly in the following.

5.2 Parent model

QuLAF is based on a state-of-the-art model, which provides input to the simplified structural tower modelling, the aerodynamic forcing and damping and the mooring description. In the present study, QuLAF is based on the FAST model already described in section 4. Hereby the switching from QuLAF to the state-of-the-art model for benchmarking of QuLAF is straightforward. The switching can also be applied in the transition from pre-design to design-verification.

5.3 Planar degrees of freedom

QuLAF solves only a 2D problem and is thus restricted to aligned wind and waves. For the load predictions this means that only the fore-aft moments and forces can be considered and that the model is not suitable for wave and wind misaligned design cases such as DLC6.2. The degrees of freedom are the platform surge, heave and pitch and the modal amplitude of the first tower mode. This is illustrated in Figure 4. The tower structural properties and first mode shape are the same as the ones given as an input to the state-of-the-art model. In the present case these are computed with the BMODES program of NREL.

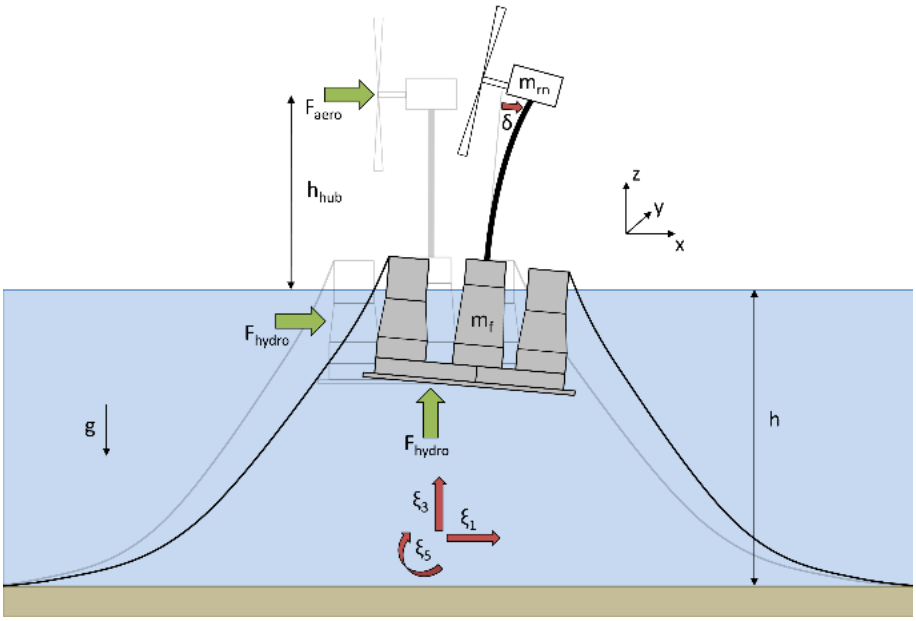

Figure 4: Sketch of the floating wind turbine as seen by the QuLAF model. From [2].

5.4 Linearized equations of motion

The equations of motion for the 3 planar floater degrees of freedom (surge, heave and pitch) are governed by (1) which are linear. In QuLAF these equations are extended by addition of the rigid wind turbine mass and inertia properties and further extended by addition of the flexible tower mode as an additional degree of freedom. The resulting equation in the frequency domain can be written

$$-\omega^2[\boldsymbol{M_{str}} + \boldsymbol{A}(\omega)]\hat{\boldsymbol{x}} + i\omega[\boldsymbol{B}_{rad}(\omega) + \boldsymbol{B}_{visc} + \boldsymbol{B}_{aero} + \boldsymbol{B}_{str}]\hat{\boldsymbol{x}} + \left[\boldsymbol{C}_{hyd} + \boldsymbol{C}_{moor} + \boldsymbol{C}_{str}\right]\hat{\boldsymbol{x}} = \hat{\boldsymbol{F}}_{aero} + \hat{\boldsymbol{F}}_{hyd} \quad (4)$$

where ω is the radian frequency, $\boldsymbol{M}_{str}$ is the structural mass matrix, $\boldsymbol{A}(\omega)$ is the hydrodynamic added mass, $\hat{\boldsymbol{x}}=[\xi_1, \xi_3, \xi_5,\delta]^T$ are the degrees of freedom, $\boldsymbol{B}_{rad}$ is the radiation damping matrix, $\boldsymbol{B}_{visc}$ is a linearized damping matrix that represents the hydrodynamic viscous damping, $\boldsymbol{B}_{aero}$ is a linear representation of the aerodynamic damping, $\boldsymbol{B}_{str}$ is the structural damping, $\boldsymbol{C}_{hyd}$ is the hydrodynamic stiffness matrix, $\boldsymbol{C}_{moor}$ is the stiffness from mooring, $\boldsymbol{C}_{str}$ is the structural stiffness, $\boldsymbol{F}_{aero}$ is the rotor load and $\boldsymbol{F}_{hyd}$ are the hydrodynamic loads.

Thus, for instance the resulting mass matrix becomes

$$\mathrm{M} = \begin{bmatrix} m_{tot} & 0 & m_{tot}z_{tot}^{CM} & m_{rn}\phi_{hub} + \sum_{i=1}^{N_t}\tilde{\rho}_i\phi_i\Delta z_i \\ & m_{tot} & 0 & 0 \\ & & I_{tot}^{O} & m_{rn}\phi_{hub}h_{hub} + I_{rn}^{TT}\phi_{z,hub} + \sum_{i=1}^{N_t}\tilde{\rho}_i\phi_i z_i\Delta z_i \\ & & & m_{rn}\phi_{hub}^2 + I_{rn}^{TT}\phi_{z,hub}^2 + \sum_{i=1}^{N_t}\tilde{\rho}_i\phi_i^2\Delta z_i \end{bmatrix} \quad (5)$$

where m_{tot} is the total mass of the floating wind turbine, which includes the mass of the floater m_f, the rotor-nacelle mass m_{rn} and the mass sum of all the elements that compose the flexible tower. The total mass inertia of the system around the flotation point O is denoted I_{tot}^{O} and includes the floater inertia I_f^O, the rotor-nacelle inertia I_{rn}^O and the inertia of each of the tower elements. z_{tot}^{CM} is the centre of mass (CM) of the whole structure and has contributions from the floater CM z_f^{CM}, the rotor-nacelle CM at the hub height h_{hub}, and the CM of each of the tower elements. The mode shape deflection of the tower evaluated at a generic tower element i is ϕ_i, while ϕ_{hub} and $\phi_{z,hub}$ are the mode shape deflection and its slope evaluated at the hub. Finally, I_{rn}^{TT} represents the mass inertia of the rotor-nacelle assembly referred to the tower top. The tower structural properties and first mode shape are the same as the ones given as an input to the state-of-the-art model.

Further, the resulting stiffness matrix becomes

$$\mathrm{C}_{struc} = \begin{bmatrix} 0 & 0 & 0 & 0 \\ & 0 & 0 & 0 \\ & & -m_{tot}gz_{tot}^{CM} & -m_{rn}g\phi_{hub} - \sum_{i=1}^{N_t}\tilde{\rho}_i g\phi_i\Delta z_i \\ & & & \sum_{i=1}^{N_t} EI_i\phi_{zz,i}^2\Delta z_i \end{bmatrix} \quad (6)$$

where g is the acceleration of gravity, and EI_i and $\phi_{zz,i}$ are the bending stiffness and the curvature of the mode shape for the tower element i, respectively. The off-diagonal term represents the negative restoring effect of the tower and rotor-nacelle mass on the tower DoF when the platform pitches.

For the mooring system, a linear mooring stiffness is calculated based on finite difference evaluations of the direct mooring loads in MoorDyn. The mooring restoring matrix C_{moor} is thus extracted from the SoA model for each mean wind speed W.

The various contributions to the terms in (4) are detailed in the following.

5.5 Hydrodynamic viscous forcing and viscous damping

The inertia-related hydrodynamic modelling is consistent with the radiation-diffraction approach in FAST and is based on the WAMIT solver. Since the equations of motion are solved in the frequency domain, there is no need for the reformulation of (1) in terms of the Cummins equation. This saves computational time and keeps the frequency dependent mass and damping properties.

The effect of viscous drag is included in the FAST model through the Morison equation. As detailed below, the viscous loads consist of both forcing and damping. In QuLAF, the viscous forcing is neglected, while the viscous damping is represented by an approximate method. This neglection of viscous forcing is thus one of the sources of discrepancy between the state-of-the-art model and QuLAF, while the damping effect is still included by an approximate method.

We now detail the division of viscous loads into forcing and damping. Consider, as an example, the horizontal viscous forcing on a vertical member from the Morison drag:

$$df = \frac{1}{2}\rho C_D D(u - \dot{x})|u - \dot{x}|dz \tag{7}$$

Here u is the horizontal wave particle velocity and $\dot{x}$ is the local structural velocity. The term can be written as

$$df = \frac{1}{2}\rho C_D D\, sgn(u - \dot{x})(u^2 - 2u\dot{x} + \dot{x}^2)dz \tag{8}$$

where the first term is the pure viscous forcing term, which would be the only term present if the structure was restrained from motion. Further, the last term is a second-order term in the structural motion. Thus under the assumption of inertia load dominance and small amplitude motion, the first and last terms can be neglected. Further assumption of $\mathrm{sgn}(u - \dot{x}) = \mathrm{sgn}(u)$ allows (8) to be re-casted as a linear damping term:

$$df_{damp} = -\rho C_D D\, |u|\dot{x}\, dz \tag{9}$$

While a full evaluation of (9) still requires integration over the full structure for each wave frequency and each active degree of freedom, the term can be further approximated by use of a central mean estimate of $|u|$. The details are given in Pegalajar-Jurado, Bredmose and Borg (2018) [2] with the final result being the global 4×4 linear damping matrix $\boldsymbol{B}_{visc}$ of (4), corresponding to the degrees of freedom of the structure shown in Figure 4. The success of this approximate damping description is part of the analysis in the present report.

5.6 Pre-computed aerodynamic forcing and damping

The aerodynamic forcing is based on the state-of-the-art FAST model and is thus precomputed for the varying wind speeds and turbulence intensities. The extraction of aerodynamic loads is done with a fixed hub in order to obtain the aerodynamic loads without the influence of the hub motion. Hereby the loads become independent of the support structure design; inertia loads are avoided; and damping effects are left out. This makes the loads re-usable for any simulation with the same wind speed, regardless of the wave conditions and the floater motion.

Thus, for each combination of wind speed and turbulence intensity the inline force, vertical force and overturning moment at the tower top was stored from a "onshore" FAST simulation and saved for later use in QuLAF. "Onshore" in this case refers to a simulation where the hydrodynamics are disabled, and the floater degrees of freedom are fixed, thus purely aerodynamic loads are extracted at hub height. The simulation time for these simulations are reduced quite significantly since the hydrodynamics are disabled. In the present study, the incident random wind and wave fields were kept the same between FAST and QuLAF to eliminate the stochastic uncertainty between different realizations.

The missing effect of the hub motion is captured by adding aerodynamic damping as a linear damping matrix to the governing equations (4). The aero-dynamic damping for each degree of freedom (surge, pitch, tower motion) was extracted in terms of decay tests for each degree of freedom for each wind speed. These decay tests were carried out in the FAST model in calm water and with the wind turbine controller active for each degree of freedom (surge, pitch, tower mode) with all the other degrees of freedom locked. This allow the floating wind turbine to be a one degree of freedom spring-mass-damper system, where the horizontal position of the hub is of interest.

The meaning "decay" is referred to as a step test in steady wind where the wind speed goes from the minimum to the maximum value, thus for every step, the structure decays to a new equilibrium position. If all sources of hydrodynamic and structural damping are disabled, the aerodynamic damping is the only responsible for the decay of the hub motion, and it can be extracted from the time series. For simplicity, the turbulence intensity was put to zero to limit the number of decay tests.

For each decay test, thus each wind speed, the equivalent linear damping ratio which delivers the same work over one oscillation cycle is extracted and the principle is based on the work done by [15]. Next for computation of the damping force,

$$b_{aero,i}(W) = 2\zeta_{aero,i}(W)\sqrt{C_{ii}(M_{ii} + A_{ii}(\omega))}, \tag{10}$$

was computed where C_{ii}, M_{ii} and $A_{ii}(\omega)$ are taken from the one-DOF oscillator in the corresponding decay test. This value can next be inserted into the global damping matrix in the equations of motion. Note that the present approach, where the damping force coefficient b is extracted rather than the damping ratio, is robust for a change of floater mass and stiffness, while the damping ratio is not. For example, if the stiffness and mass were both doubled, the natural frequency would remain unchanged, while the damping ratio would decrease by a factor of 2, although the aerodynamic damping load represented by $b_{aero,i}(W)$ would be unchanged. For this reason b is transferred for the decay test to preserve the validity of the damping for various floater designs.

5.7 Frequency domain motion solver

Due to the linearity of all equations of motion (4), solution in the frequency domain is possible. Thus, for a given rotor load time series and a given wave time series, the forcing is transformed to the fre-

quency domain by FFT and the coupled linear equation system is solved at each frequency. Back-transformation to the time domain is done with IFFT, thus eliminating the need for explicit time domain integration of the equations of motion.

5.8 Static offset

The frequency domain approach is based on linearization around the equilibrium position for each wind speed and under the assumption of small displacements around the equilibrium position. The equations of motion are thus solved for the fluctuations around this equilibrium. The total deflection is thus the sum of the equilibrium position and the fluctuations. Therefore, when QuLAF is initialized, the offset at each wind speed is computed as part of the linearization and is eventually included in the total response output.

5.9 Summary of model limitations

QuLAF is intended so solve the same governing equations as a full state-of-the-art model solves. Some approximations, though, have been made to allow for the linearization and fast solution in the frequency domain. Prior to the present study, a smaller set of results with the QuLAF model has been presented in [2]. From this study – and confirmed by the present results – the main limitations of QuLAF can be summarized as

A. An under-prediction of the wave excitation force at large sea states due to the omission of viscous drag forcing. This is explained in section 5.5 and leads to under-prediction of surge and pitch for strong sea states.
B. An under-prediction of the wind-induced response around rated wind speed, where the controller in the full FAST model switches between the partial-load (torque control; fixed blade pitch) and full-load (varying blade pitch; fixed target shaft speed). Due to the structural motion in the state-of-the-art model, the turbine will experience a larger fluctuation for the apparent nacelle wind speed. The controller will react to this and the resulting thrust is reduced relative to the nominal steady thrust at rated wind speed. For the pre-calculation of rotor loads with a fixed nacelle, the apparent wind speed is closer to rated and the resulting thrust is also closer to the nominal thrust.
C. An under-predicted nacelle acceleration due to over-predicted aerodynamic damping for the tower mode motion (at 0.682 Hz). Initial results indicate that the damping decreases with frequency. Since the damping of the decay test is based on a clamped tower with rigid blades, the natural frequency of this is (0.51 Hz) lower and thus leads to a larger damping than at the coupled tower frequency. In comparison the full FAST model has a coupled tower frequency of 0.746 Hz when moored and with flexible blades.

While all of these limitations may be compensated by model calibration, we have decided to keep the generic model formulation and leave this potential for later exploitation. It should be noted that further tuning of the model will always be concept-specific and may thus introduce a bias in the model which may not be generally applicable.

5.10 Summary: What is needed to run the model

Since QuLAF shares several inputs and calculations and even pre-calculations with the state-of-the-art model, we here summarize what is needed to run the model. The model application can be divided into a preparation step and a calculation step. The latter can be done repeatedly for many substructure candidates and is the step where the speed benefit relative to the state-of-the-art model is advantageous.

Preparation: Given the turbine and design basis and reference floater design:

- Calculate time series of rotor forcing for a fixed nacelle and stiff blades at the needed wind speeds and for the needed length and number of seeds. Apply a controller that is tuned to the platform pitch frequency of the reference floater.
- Carry out decay tests for the surge, pitch and clamped tower degrees of freedom.
- The results are saved in a data base and can be re-used for many candidate designs

Calculation (pre-design loop): For each new candidate floater design:

- Compute the radiation-diffraction solution in WAMIT
- Extract the structural mass and stiffness properties
- At each wind speed calculate the equilibrium position and linearize the mooring stiffness around this point
- Run QuLAF to get an efficient prediction of the fatigue and ULS response.

The benefit of QuLAF is thus the efficient calculation of the last step for many candidates designs and for quicker load analysis. Compared to straight application of a state-of-the-art model, the only extra computations needed to achieve this speed up are the rotor decay tests in the preparation step and the mooring linearization in the pre-design loop.

After a pre-design has been settled, the design should be verified for the complete load basis in a state-of-the-art model, following the design codes.

6 Results

The QuLAF and FAST results from the load cases, presented in Table 2, can now be analysed, compared and discussed. This section will present the fatigue limit states (FLS) analysis and ultimate limit state (ULS) analysis. Each displaying the design load and response values for different parts of the floating wind turbine, i.e. nacelle acceleration, tower base bending moment, surge, heave and pitch motion of the floater. In the fatigue analysis the damage-equivalent loads (DELs) will be presented and they were computed from the load time series for each simulation separately by applying a rain-flow counting method. These results are followed by a table presenting the DELs where the weighting of the different wind speeds and peak periods according to the assumed Weibull distribution and probabilities (given in D7.2 [16]), has been considered.

In general, the design load and response values for both the simplified model (QuLAF) and the SoA model (FAST) will be presented as function of environmental conditions which in this study will be conditioned on wind speed. This also means that wave heights and periods are all conditioned on the wind speed. In addition, to more easily compare the load prediction of the two models, corresponding quantile-quantile (Q-Q) plots are also presented. Furthermore, boxplots are used to describe spread and median of the ratio between the damage-equivalent or maximum values from QuLAF and FAST. The boxplots show the minimum, first quantile, median (line in the center of the box), third quantile and the maximum of the data for each wind speed. The mean values of the response ratios in the ULS analysis are then presented in an associated table.

Finally, in the ULS summary an overview of the ultimate load and response populations are presented in a boxplot for each of the design load cases. This way the critical cases can be appointed and compared for the two models. The ultimate load and response values presented in the summary plots are obtained as a mean of all the maximum values for each seed associated to the specific environmental condition. Also, it should be noted that the wind speed values on the figures refer to the mean speed at hub height.

In the following discussion of the results the simplified model QuLAF will be the point of reference when compared to FAST. This means that for example if the results are generally under-predicted it is QuLAF that is under-predicting compared to FAST.

6.1 FLS simulation study

The fatigue DEL nacelle acceleration and tower base bending moment for FAST and QuLAF are shown in Figure 5 as function of environmental conditions together with the corresponding Q-Q plot. Figure 6 presents the QuLAF/ FAST-ratios of the fatigue DELs. Table 5 shows DELs based on the weighting of the different wind speeds according to the assumed Weibull distribution and probabilities of [16].

Again, it should be pointed out that the nacelle acceleration is not really a DEL, but analysed with the rain-flow counting method and presented as DEL.

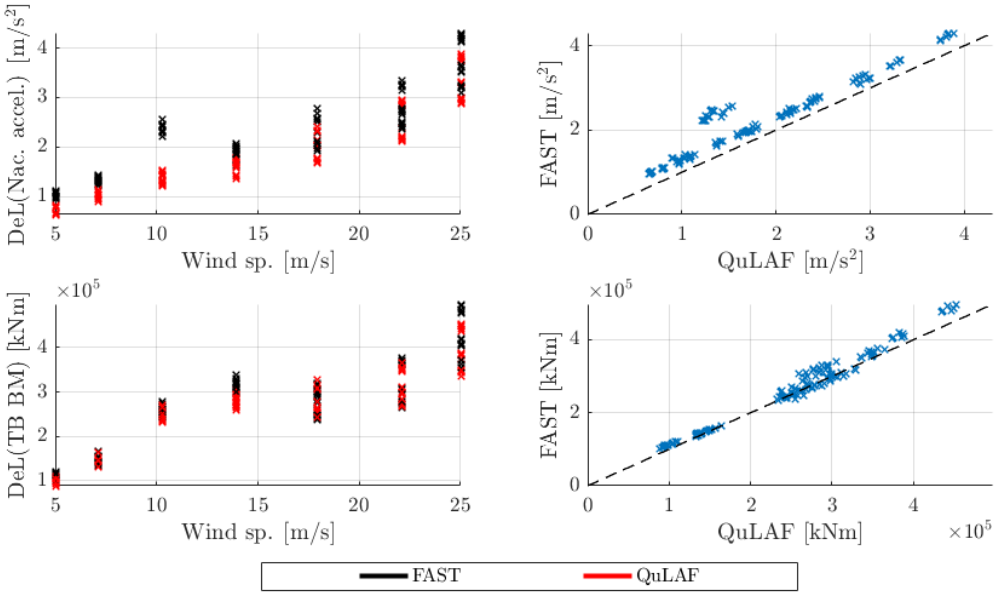

Figure 5: Fatigue damage-equivalent nacelle acceleration and bending moment at the tower base for DLC1.2.

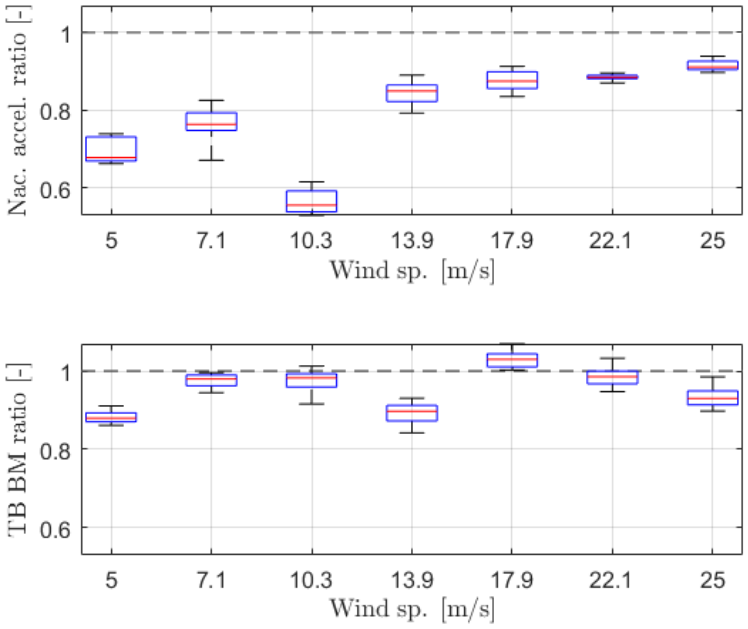

Figure 6: QuLAF/ FAST-ratios of the fatigue DELs (Nacelle acceleration and tower base bending moment) for DLC1.2 displayed in boxplots

Table 5: FAST and QuLAF DEL results based on probabilities from the Weibull distribution of NSS [16].

	FAST	*QuLAF*	*ratio*
DEL: Nac. accel. [m/s^2]	1.86	1.38	0.74
DEL: TB BM [kNm]	$2.29 \cdot 10^5$	$2.18 \cdot 10^5$	0.95

Based on the results presented in Figure 5 and Figure 6 together with Table 5, the following findings can be summarized:

- Nacelle acceleration: The results show a general under-prediction in QuLAF which is due to the nacelle acceleration being governed by the wind forcing, resulting in and enhanced effect of three limitations; the complex environment around rated conditions makes the controller behave differently in the two models, the assumption of rigid blades lowers the coupled tower natural frequency and lastly that the aerodynamic damping is extracted from a not floating case. See all limitations in Section 5.9. This also explains the distinct deviation at 10.3m/s which is highly affected by the controller-transition, see limitation B in Section 5.9. The largest DEL is observed at highest environmental state, i.e. 25 m/s, with a 20% under-prediction. One should note that the highest DEL would be at rated conditions if the probabilities from the Weibull distribution had been included in the plots.
- Tower base bending moment: An overall good agreement between the two models is observed but with a slight DEL under-prediction of QuLAF just above rated conditions and at cut-out.
- Overall: From the FAST and QuLAF DEL results, where the probabilities from the Weibull distribution has been taken into account, it is seen that QuLAF under-predicts the DEL nacelle acceleration by 26%, but only 5% for the tower base bending moment. The under-prediction of nacelle acceleration can be explained to limitation B of section 5.9 where the tower top aerodynamic damping is over-predicted.

6.2 ULS simulation study

6.2.1 DLC1.2 – baseline

DLC1.2 (a fatigue DLC) is included in the ULS analysis since it serves as a baseline case for the other DLCs, since normal conditions are considered, i.e. NTM and NSS. This way it is easy to understand the response change between the models when either adding extreme turbulence (DLC1.3) or severe sea states (DLC1.6).

The nacelle acceleration, tower base bending moment and planar motions of the floater are shown in Figure 7 as function of environmental conditions together with the corresponding Q-Q plot. Figure 8 presents the QuLAF/ FAST-ratios of the max. values.

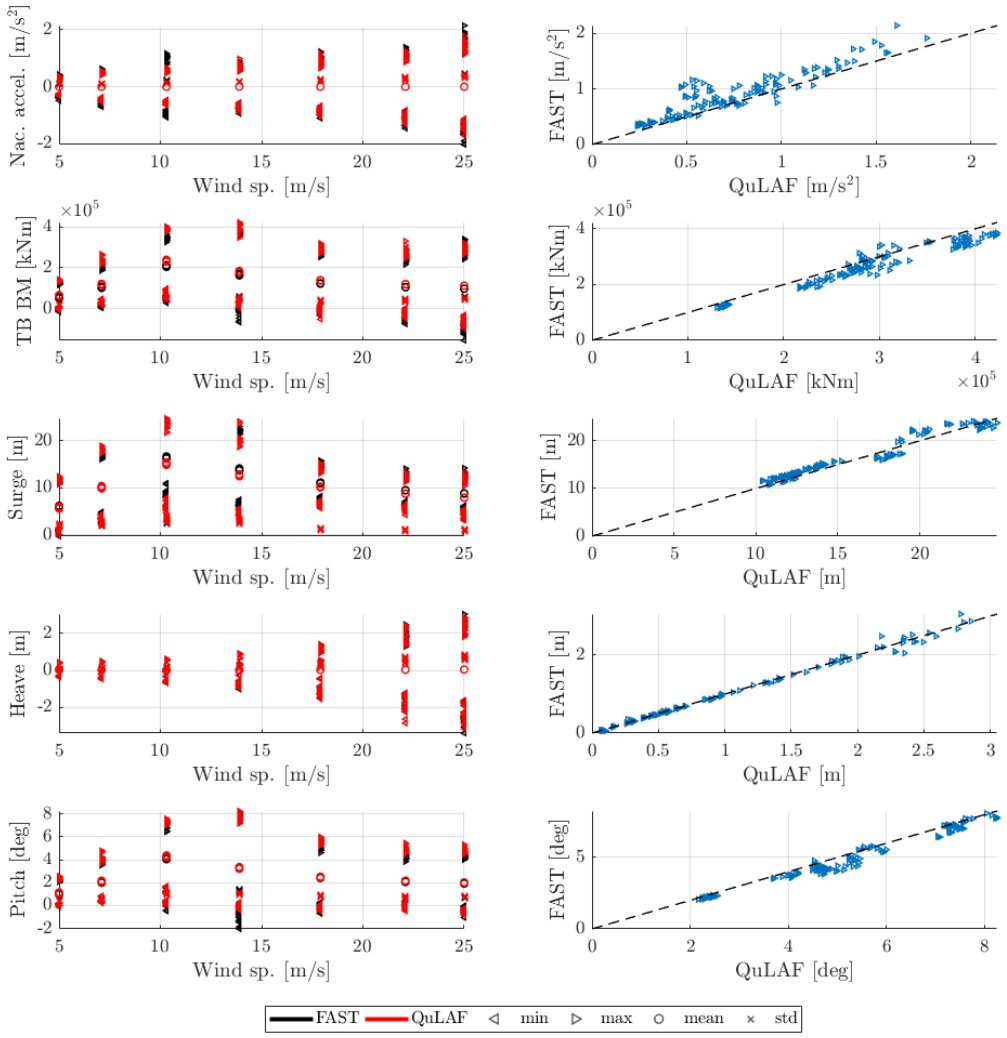

Figure 7: Response to DLC1.2 for FAST and QuLAF. Left: min., max., mean and std. values for every realisation as function of wind speed. Right: maximum values for FAST as function of the corresponding maximum values in QuLAF

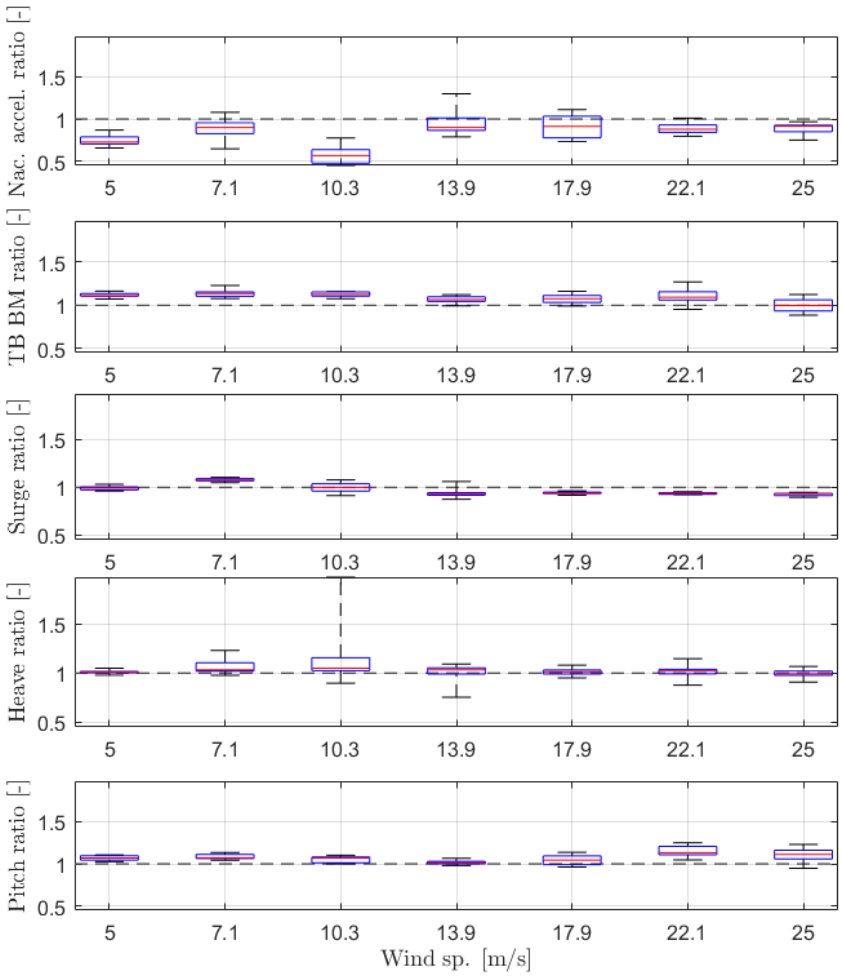

Figure 8: QuLAF/ FAST-ratios of the max. values for DLC1.2 displayed in boxplots

Table 6: Mean values of the response ratios of the max. values for DLC1.2.

Mean(X_{QuLAF}/X_{FAST}) [-]	**Wind speed [m/s]**						
	5	7.1	10.3	13.9	17.9	22.1	25
Nac. Accel.	0.75	0.88	0.57	0.94	0.90	0.89	0.89
TB BM	1.12	1.14	1.13	1.07	1.08	1.11	1.00
Surge	0.99	1.08	0.99	0.95	0.94	0.94	0.93
Heave	1.01	1.06	1.15	1.01	1.01	1.02	0.99
Pitch	1.07	1.08	1.05	1.02	1.05	1.14	1.10

Based on the results presented in Figure 7 and Figure 8 together with Table 6, the following findings can be summarized:

- Nacelle acceleration: The largest value is obtained at 25 m/s with an 11% under-prediction. This can be linked to an over-predicted aero-dynamic damping of the tower top motion, see section 5.9.
- Tower base bending moment: The largest value is obtained around rated conditions with a 13% over-prediction.
- Surge motion: Largest response is observed around rated conditions with an under-prediction of 1-5%.

- Heave motion: The response is governed by the waves, i.e. achieves the largest value at 25 m/s with an under-prediction of 1%.
- Pitch motion: The pitch response is governed by wind forcing, i.e. largest at rated with an over-prediction of 2%.

6.2.2 DLC1.3

The nacelle acceleration, tower base bending moment and planar motions of the floater are shown in Figure 9 as function of environmental conditions together with the corresponding Q-Q plot. Figure 10 presents the QuLAF/ FAST-ratios of the max. values.

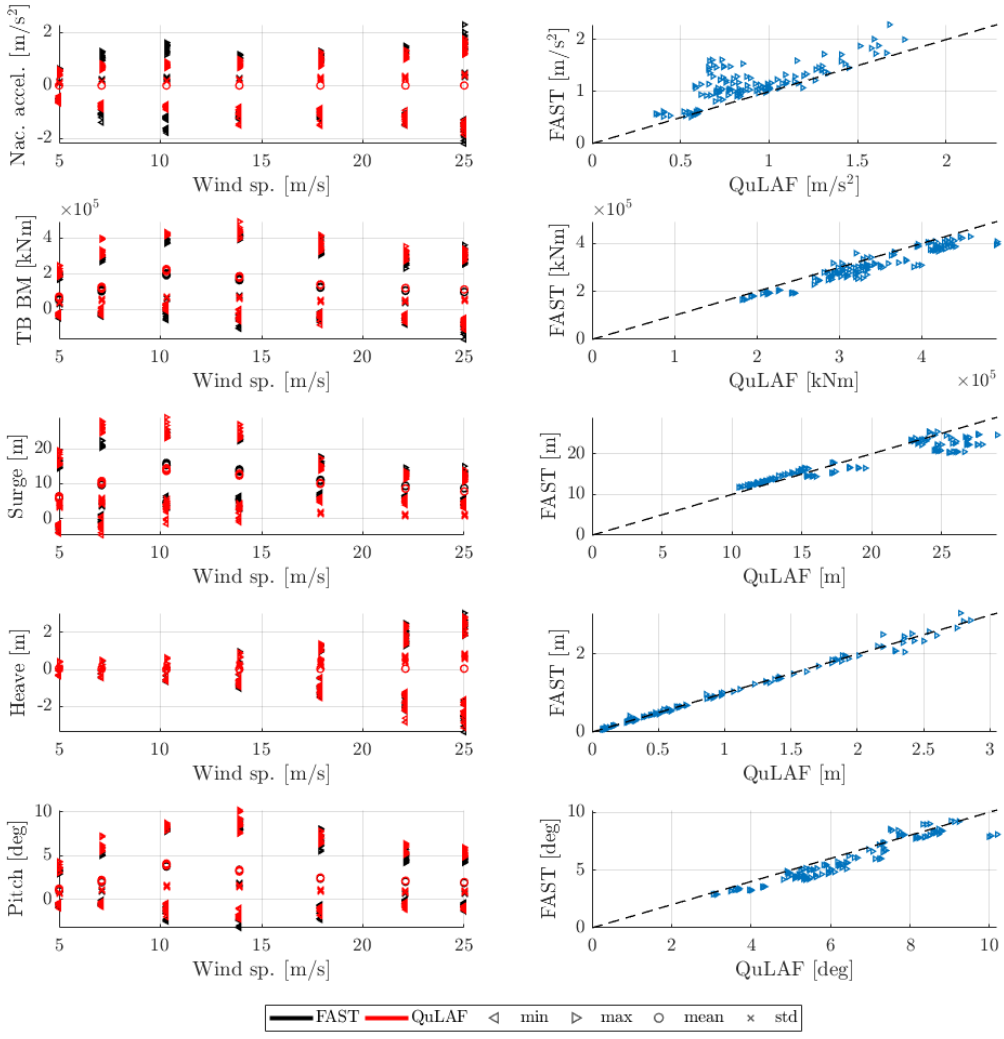

Figure 9: Response to DLC1.3 for FAST and QuLAF. Left: min., max., mean and std. values for every realisation as function of wind speed. Right: maximum values for FAST as function of the corresponding maximum values in QuLAF

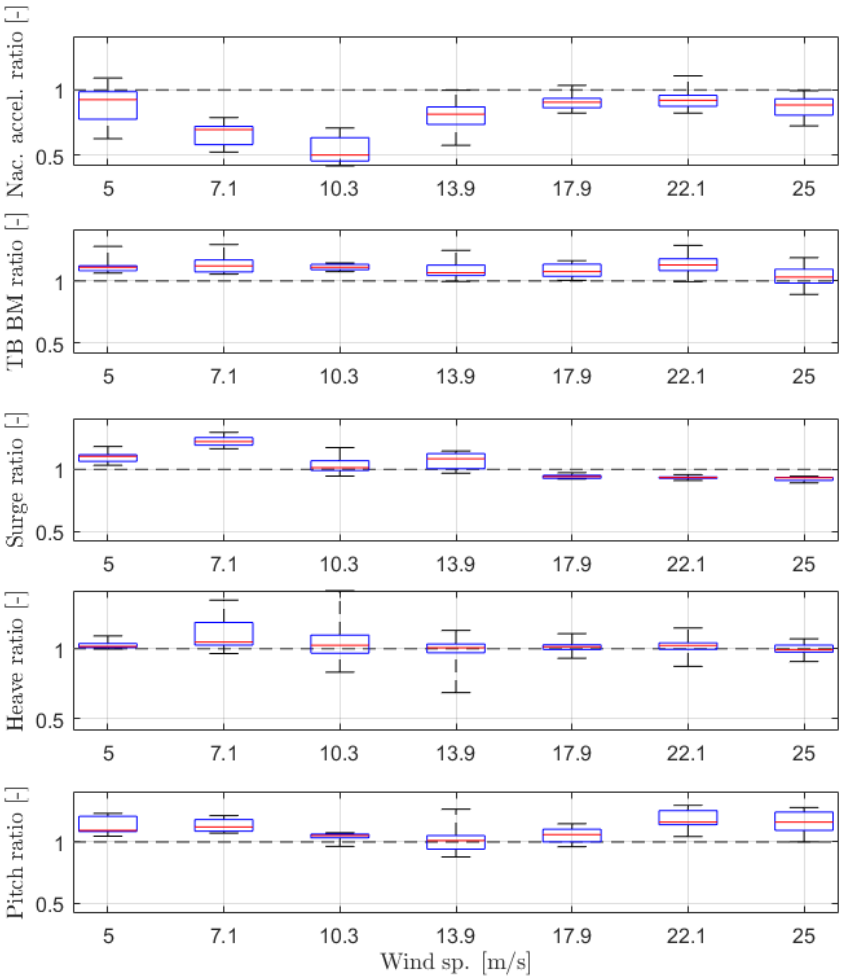

Figure 10: QuLAF/ FAST-ratios of the max. values for DLC1.3 displayed in boxplots

Table 7: Mean values of the response ratios of the max. values for DLC1.3.

Mean(X_{QuLAF}/X_{FAST}) [-]	**Wind speed [m/s]**						
	5	7.1	10.3	13.9	17.9	22.1	25
Nac. Accel.	0.88	0.66	0.53	0.80	0.91	0.93	0.87
TB BM	1.13	1.14	1.11	1.09	1.08	1.14	1.04
Surge	1.10	1.22	1.03	1.07	0.94	0.93	0.92
Heave	1.03	1.10	1.04	0.98	1.01	1.02	1.00
Pitch	1.13	1.13	1.04	1.03	1.06	1.17	1.16

Based on the results presented in Figure 9 and Figure 10 together with Table 7, the following findings can be summarized:

- Overall: It is observed that the wind forcing dominates more at low wind compared DLC1.2. The extreme turbulence enhances the effect of the limitation B in Section 5.9 by making expanding the area where the controller switches between region 1 and 2, especially below rated conditions. This can be seen as a high over-prediction in surge and pitch at 7.1 m/s, while an under-prediction of the nacelle acceleration.
- Nacelle acceleration: The largest value is obtained at rated conditions with a severe under-prediction of 47%.
- Tower base bending moment: As for DLC1.2 the largest load is obtained at rated conditions with the same level of over-prediction of 11%.

- Surge motion: The largest response is achieved at rated conditions with a 3% over-prediction – although a 22% over-prediction at 7.1 m/s
- Heave motion: As for DLC12 the responses from the two models agree very well and largest at cut-out.
- Pitch motion: Achieves largest response just above rated as for DLC1.2 with a slight over-prediction of 3%.

6.2.3 DLC1.6

The nacelle acceleration, tower base bending moment and planar motions of the floater are shown in Figure 11 as function of environmental conditions together with the corresponding Q-Q plot. Figure 12 presents the QuLAF/ FAST-ratios of the max. values.

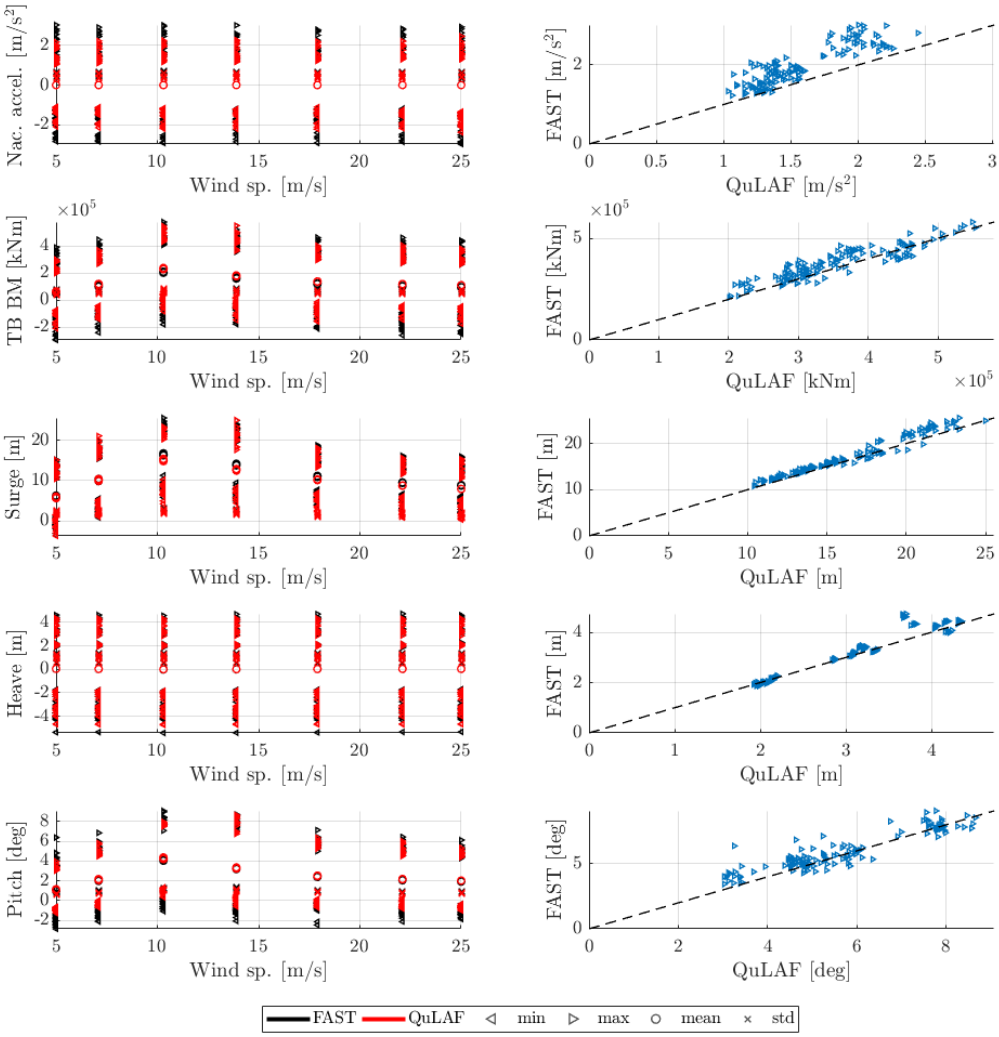

Figure 11: Response to DLC1.6 for FAST and QuLAF. Left: min., max., mean and std. values for every realisation as function of wind speed. Right: maximum values for FAST as function of the corresponding maximum values in QuLAF

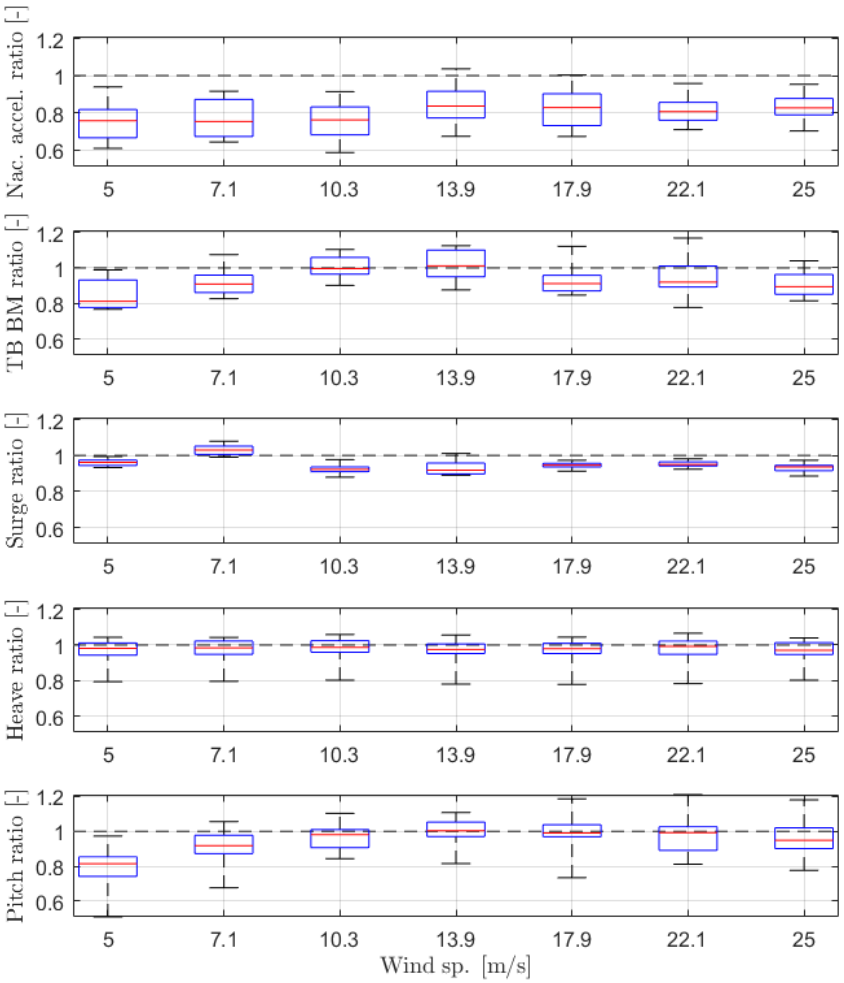

Figure 12: QuLAF/ FAST-ratios of the max. values for DLC1.6 displayed in boxplots

Table 8: Mean values of the response ratios of the max. values for DLC1.6.

Mean(X_{QuLAF}/X_{FAST})	**Wind speed [m/s]**						
	5	7.1	10.3	13.9	17.9	22.1	25
Nac. Accel.	0.75	0.75	0.77	0.84	0.83	0.82	0.84
TB BM	0.85	0.92	1.00	1.01	0.93	0.94	0.91
Surge	0.96	1.03	0.92	0.93	0.95	0.95	0.93
Heave	0.97	0.97	0.98	0.97	0.97	0.98	0.97
Pitch	0.80	0.92	0.97	1.00	0.99	0.98	0.97

Based on the results presented in Figure 11 and Figure 12 together with Table 8, the following findings can be summarized:

- Overall: Compared to DLC1.2 the results are now more wave dominated, so the max response values are more uniform over the wind speeds due to the fact that SSS is assumed to use the parameters corresponding to ESS [16], which are applied for all wind speeds.
- Nacelle acceleration: The maximum values are wave dominated, hence uniform over the wind speed, but generally under-predicted up to 25%, which is due to limitation C in Section 5.9.
- Tower base bending moment: The largest load is obtained at rated and is matched perfectly by QuLAF.

- Surge motion: The largest response is obtained around rated conditions with a 7-8% under-prediction. This deviation is due to the missing viscous drag in QuLAF, i.e. limitation A in Section 5.9.
- Heave motion: As the heave response is governed by the waves the values are uniform and with a typical under-prediction of 3%.
- Pitch motion: The pitch response is more wind dominated, thus largest close to rated conditions with 0-3% under-prediction. It can also be observed that the combination of larger waves and under-prediction caused by limitation A in Section 5.9 actually repairs the deviation between QuLAF and FAST above rated conditions.

6.2.4 DLC2.1

The nacelle acceleration, tower base bending moment and planar motions of the floater are shown in Figure 13 as function of environmental conditions together with the corresponding Q-Q plot. Figure 14 presents the QuLAF/ FAST-ratios of the max. values.

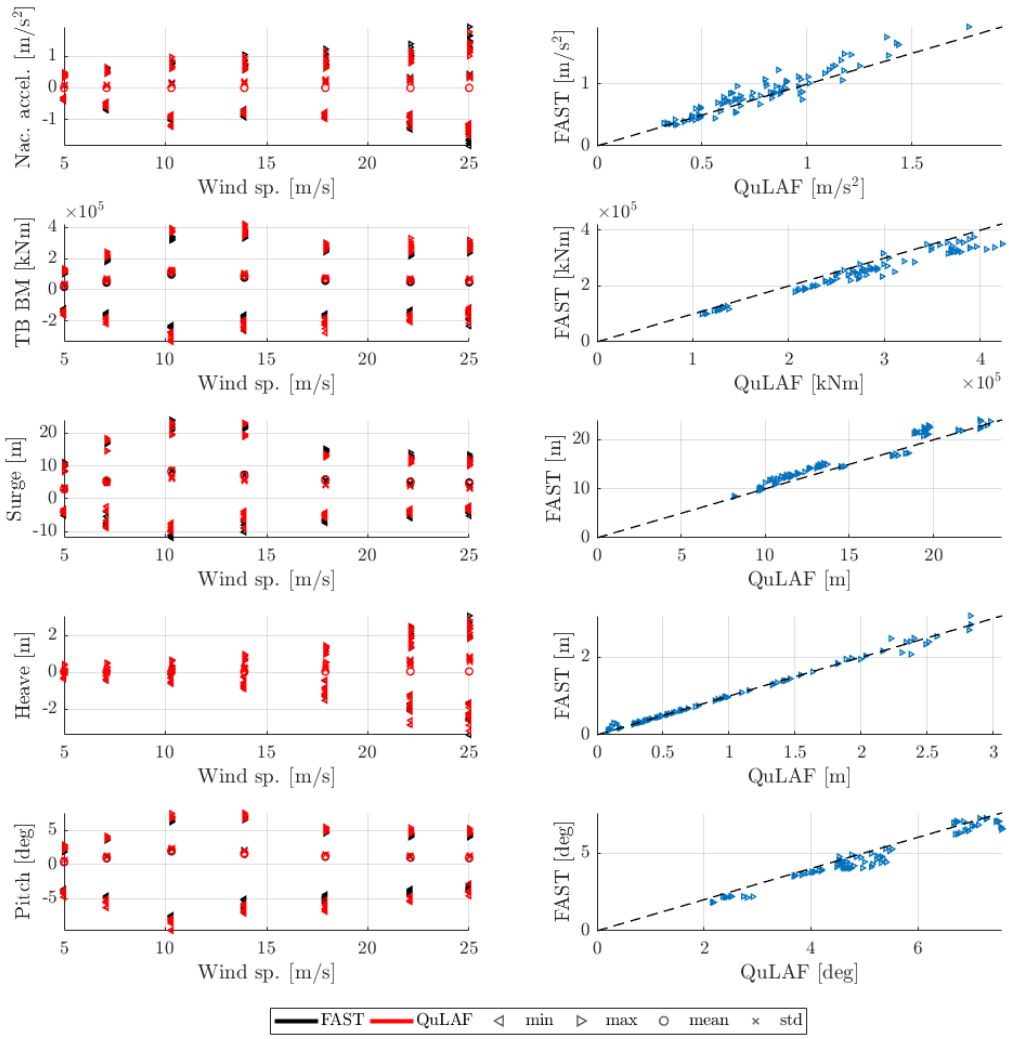

Figure 13: Response to DLC2.1 for FAST and QuLAF. Left: min., max., mean and std. values for every realisation as function of wind speed. Right: maximum values for FAST as function of the corresponding maximum values in QuLAF

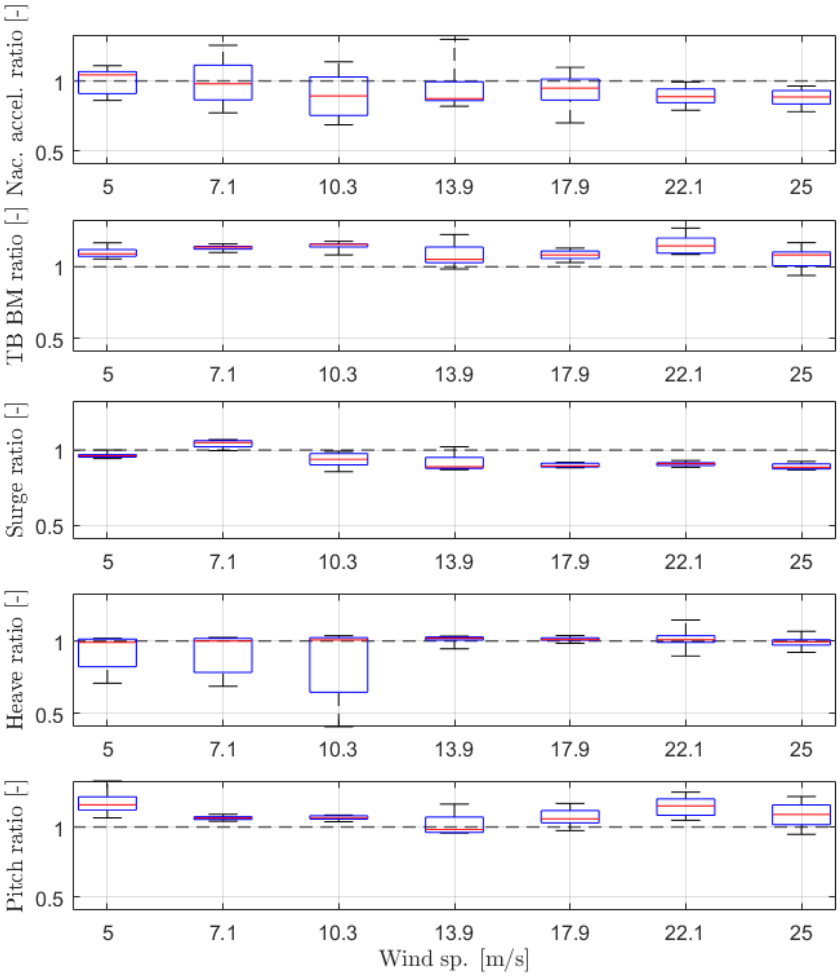

Figure 14: QuLAF/ FAST-ratios of the max. values for DLC2.1 displayed in boxplots

Table 9: Mean values of the response ratios of the max. values for DLC2.1.

Mean(X_{QuLAF}/X_{FAST})	**Wind speed [m/s]**						
	5	7.1	10.3	13.9	17.9	22.1	25
Nac. Accel.	1.00	0.99	0.91	0.94	0.93	0.90	0.88
TB BM	1.10	1.13	1.15	1.08	1.08	1.15	1.06
Surge	0.96	1.04	0.93	0.92	0.90	0.91	0.89
Heave	0.93	0.92	0.86	1.01	1.01	1.02	0.99
Pitch	1.17	1.06	1.07	1.02	1.07	1.14	1.09

Based on the results presented in Figure 13 and Figure 14 together with Table 9, the following findings can be summarized:

- Overall: very similar to DLC1.2 and DLC1.3, but only maximum values have been considered, which might not be representative for this transient load case, where also the negative values have influence.
- Nacelle acceleration: As in DLC1.2 the largest value is obtained at cut-out with a 12% under-prediction.
- Tower base bending moment: Similar to DLC1.2 the largest load is observed around rated conditions with an over-prediction of 8-15%.
- Surge motion: The largest values are achieved around rated as in DLC1.2, but with a slightly higher under-prediction of 7-8%.
- Heave and pitch motion: match very well the results from DLC1.2

6.2.5 DLC6.1

The nacelle acceleration, tower base bending moment and planar motions of the floater are shown in Figure 15 as function of environmental conditions together with the corresponding Q-Q plot. Figure 16 presents the QuLAF/ FAST-ratios of the max. values.

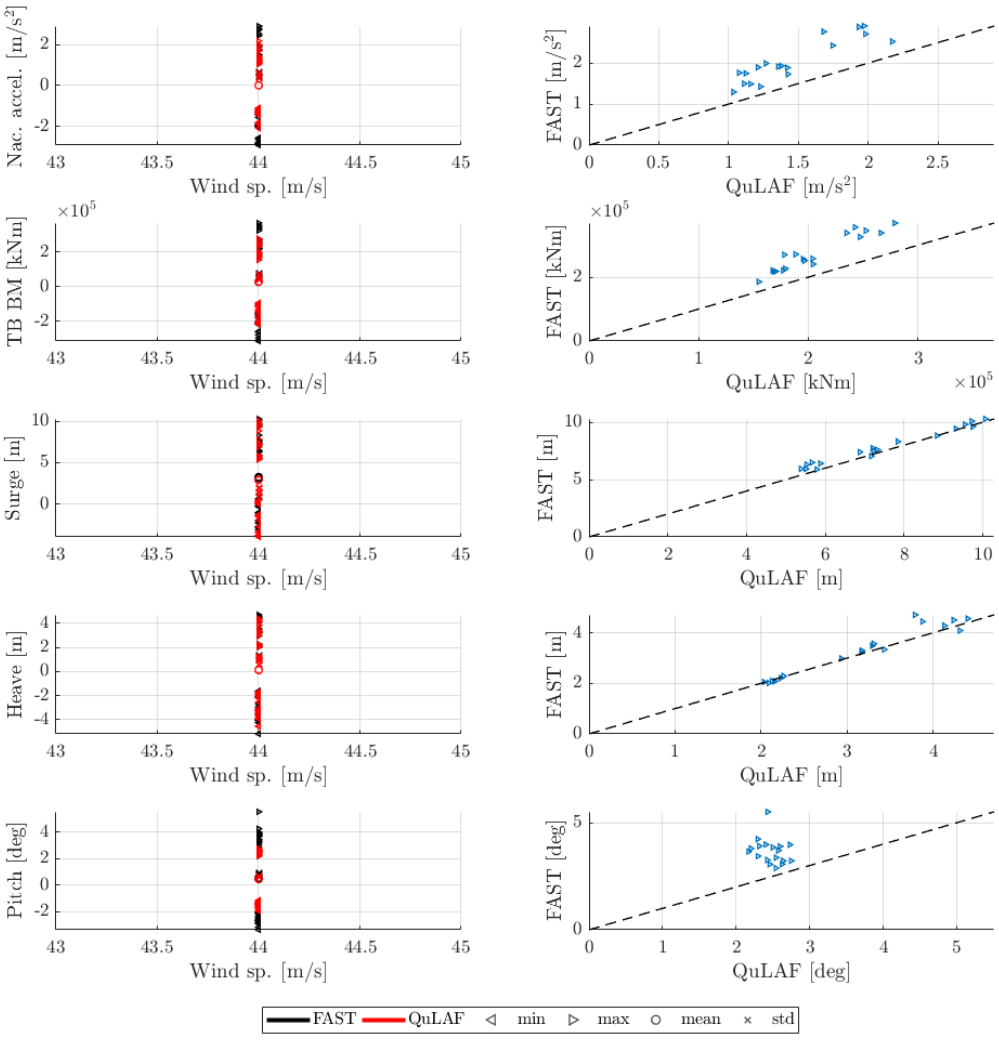

Figure 15: Response to DLC6.1 for FAST and QuLAF. Left: min., max., mean and std. values for every realisation as function of wind speed. Right: maximum values for FAST as function of the corresponding maximum values in QuLAF

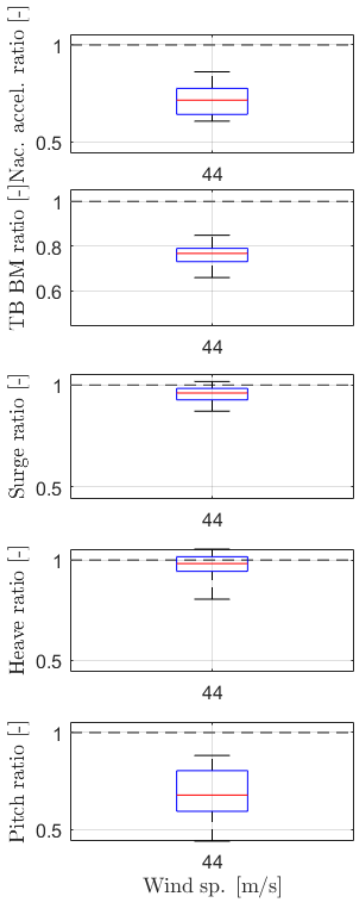

Figure 16: QuLAF/ FAST-ratios of the max. values for DLC6.1 displayed in boxplots

Table 10: Mean values of the response ratios of the max. values for DLC6.1.

Mean(X_{QuLAF}/X_{FAST})	**Wind speed [m/s]** 44
Nac. Accel.	0.72
TB BM	0.76
Surge	0.95
Heave	0.97
Pitch	0.69

Based on the results presented in Figure 15 and Figure 16 together with Table 10, the following findings can be summarized:

- Overall: the results correspond to DLC1.6 at 5 m/s, since the thrust level is nearly the same and both load cases utilises the extreme sea state. Generally, an under-prediction can be seen on all the values which is due to the limitation of A in Section 5.9 regarding the missing viscous wave effects.

6.2.6 Summary of ULS analysis

The population of maximum values of the nacelle acceleration, tower bending moment and planar motions for each of the five load cases are presented in Figure 17. Based on the results presented in the figure, the following findings can be summarized:

- The ultimate nacelle accelerations are governed by the extreme sea state (DLC1.6 and DLC6.1). Both model agree on this conclusion but with an under-prediction of the values in QuLAF.
- The ultimate tower base bending moments are obtained in DLC1.6 and both models agree very well on the values.
- The largest surge motions are obtained in DLC1.3 with a slight over-prediction of the loads in QuLAF.
- The largest heave motions are generally very well matched in QuLAF and since they are governed by the waves the governing load cases are the ESS cases.
- The largest pitch motions would have been achieved in DLC2.1 if the negative values had been considered. However since only the maximum values have been investigated the largest responses are obtained in DLC1.3 and DLC1.6.

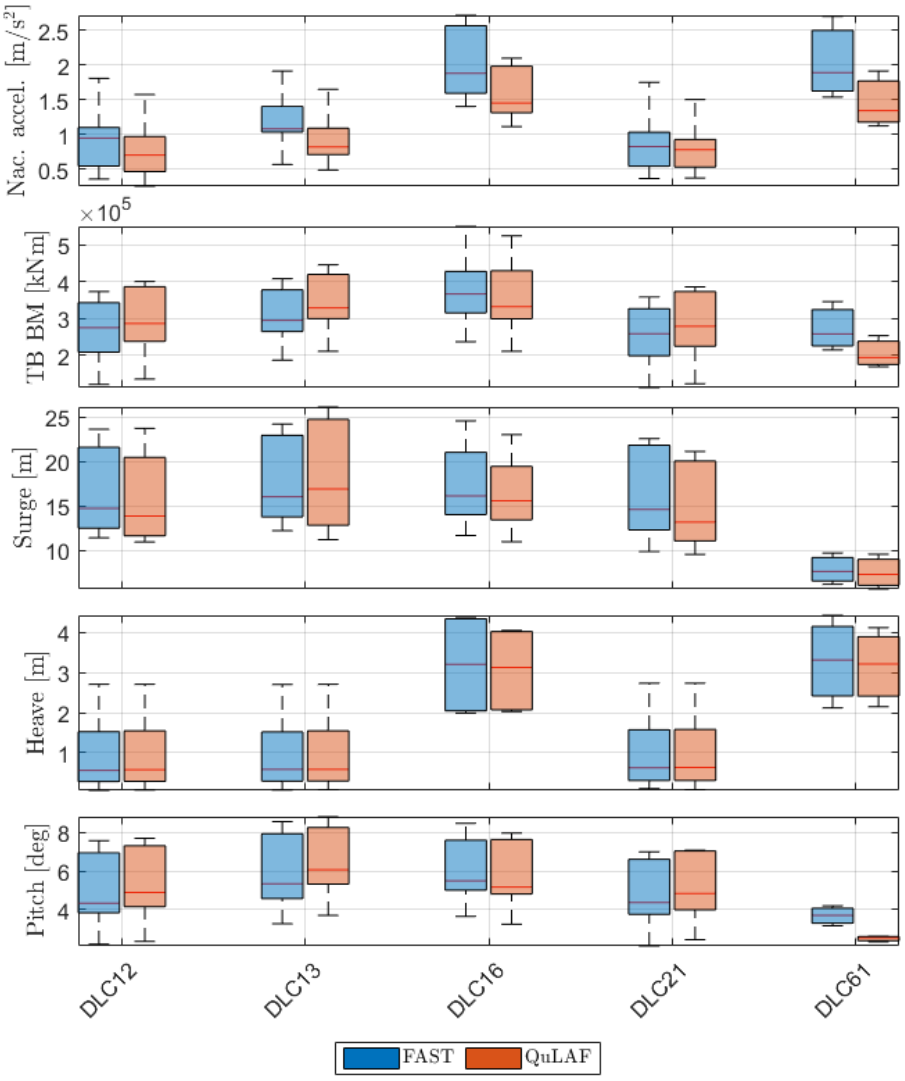

Figure 17: Population of max. values for each of the five load cases.

In order to see if the models predict the same design-driving cases, the ranking of the eight highest maximum values of the nacelle acceleration, tower base bending moment and planar motions with their corresponding load case simulations are presented in Figure 18-Figure 22. Based on the results presented in the figures, the following findings can be summarized:

- Nacelle acceleration: The values are under-predicted, but the two models agree on the same governing load cases.
- Tower base bending moment: The two models agree very well in both maximum values and load cases. The maximum tower bending moments for both models are obtained in severe sea states around rated wind speed.
- Surge motion: Overall both models predict that the highest surge motion is obtained in extreme turbulence just below rated wind speed. Generally good agreement but with a slight over-prediction in QuLAF.
- Heave motion: Always a good agreement as FAST and QuLAF since the relative velocity is small.
- Pitch motion: Overall very well agreement between the two models. They both predict that the largest pitch motions are obtained in extreme turbulence conditions around rated wind speed.
- Overall: The load levels are generally in good agreement and the differences are smaller than it appears from Figure 17. This means that the model differences between FAST and QuLAF compensate for each other when looking at the overall maximum loads in the global ULS analysis.

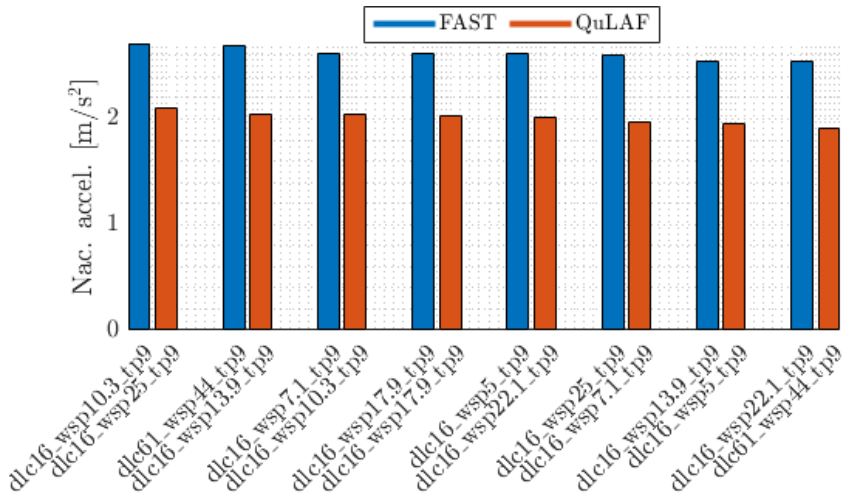

Figure 18: Ranking of the eight highest max. values of the nacelle acceleration and corresponding load case simulations for FAST and QuLAF

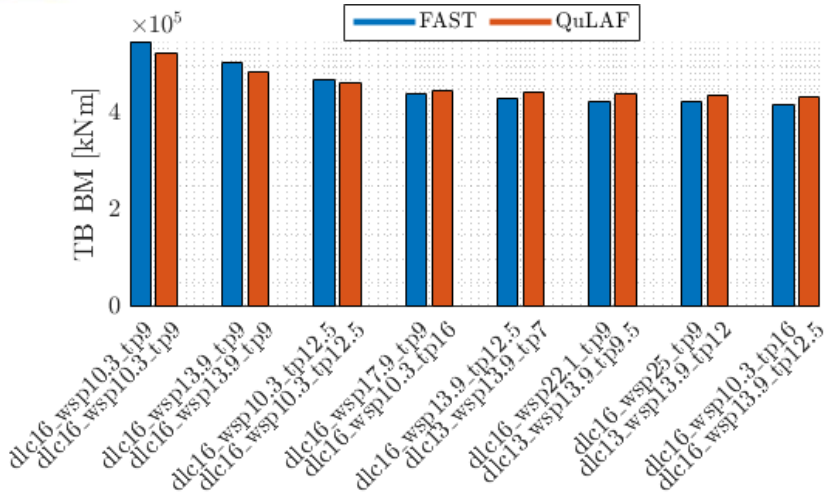

Figure 20: Ranking of the eight highest max. values of the tower base bending moment and corresponding load case simulations for FAST and QuLAF

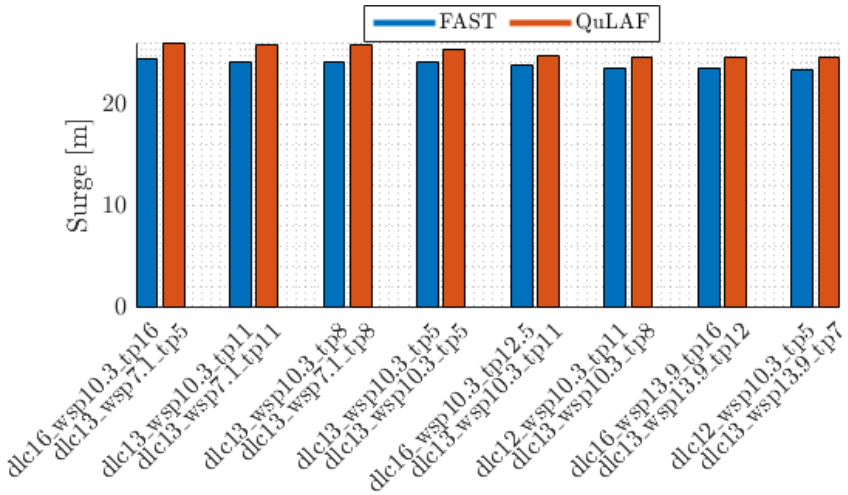

Figure 21: Ranking of the eight highest max. values of the surge motion and corresponding load case simulations for FAST and QuLAF

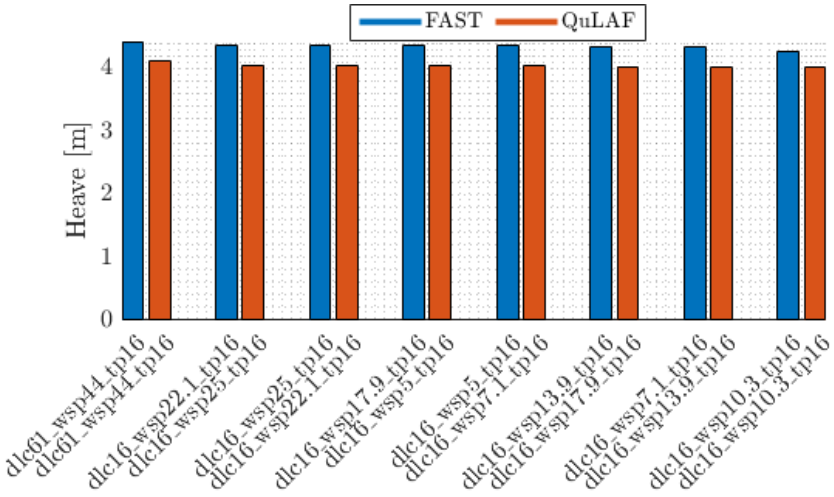

Figure 22: Ranking of the eight highest max. values of the heave motion and corresponding load case simulations for FAST and QuLAF

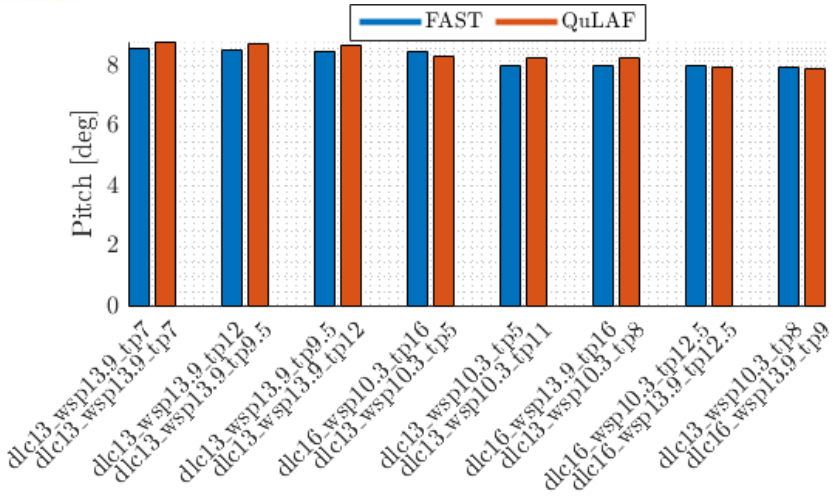

Figure 22: Ranking of the eight highest max. values of the pitch motion and corresponding load case simulations for FAST and QuLAF

7 Design Practice of Floating Wind Turbines

In previous work as part of LIFES50+, a state-of-the-art of the design practice of floating wind turbines with different generalized design stages was assessed. As described in the introductory section and shown in Figure 7.1, simplified models are an important part in the early stages of the design. Floating wind turbine design is extremely complex due to many possible variations and thus typically needs many iterations in order to arrive at a feasible solution for a given site.

From an industry perspective, the application of simplified tools such as QuLAF is confined to the early conceptual project stages. Primarily in the optimization phase, checking and comparing different sub-structure and mooring configurations, such methods are very useful to obtain improved understanding of the influences of design parameters – much improved over e.g. simple static calculations or running only few individual load simulations. Also, there is an application of such models with respect to control system design, as models of the QuLAF-type is linear and thus can be included in classical controller design methodologies.

In the first stage (conceptual design), the main goal is to obtain a resilient solution that is only slightly varied in the more detailed design stages. However, at the beginning of the design process, it is extremely important to reduce the complexity of the variable space. The most important decisions to make are to identify the best-suited concept (e.g. tension leg, spar, semi-submersible, etc.), concept variation (e.g. platform/mooring line material, number of columns / pontoons / mooring lines, etc.) and concept parameters (dimensions of principle platform components) for a given site. Because the goal of this optimization procedure is not to determine the exact loading but only the variation that will perform best, simplified models, which are able to capture the severity of different load cases, support the designer in deciding for a certain design over another. In this stage, it is also important to derive a general feasibility of a concept for a given site and determine some estimated cost of the system. Here, simplified models can help to increase the accuracy of the estimations through determining the most severe load cases of the concept. Based on these design driving load cases it is possible to perform a faster pre-design by only simulating few simulations with e.g. FAST. In this way, simplified models add substantial value (through an added step of fidelity) to the generally used spreadsheet design procedures in the conceptual design stage.

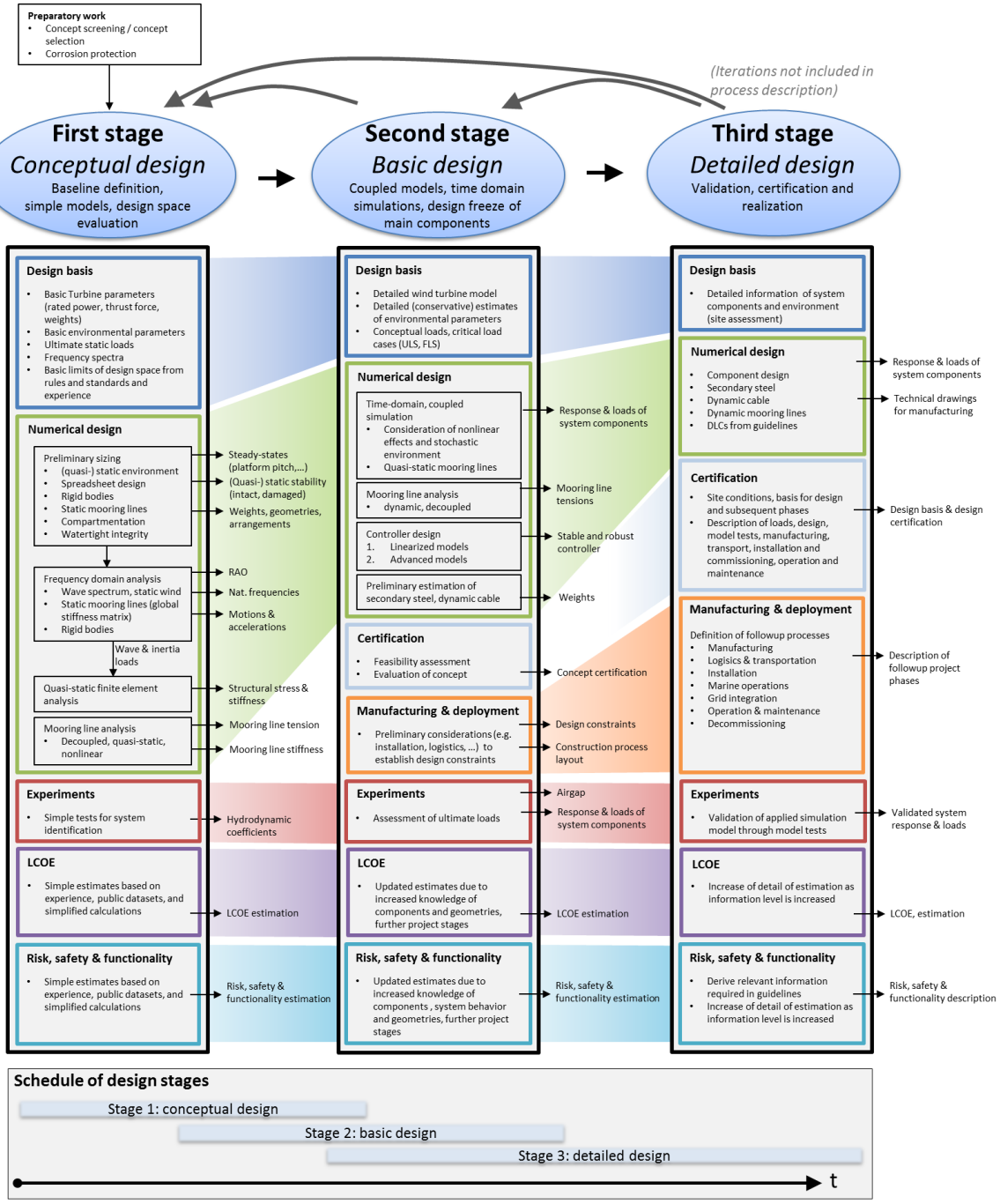

Figure 7.1: Design stage overview [17]

In the **second stage (basic design)**, the goal is to obtain reliable load responses for a given concept (which was determined in the first design stage) across all load scenarios that are expected throughout the lifetime of the system. These are performed with medium fidelity tools such as FAST and can be considered as a design verification as it is not expected that the design will be changed significantly at this stage. This is because experimental tests, manufacturing, and certification are initialized in this stage and each iteration loop is increasingly expensive. The results from the medium fidelity tools also serve as input for more detailed simulations (e.g. determined worst-case scenario resulting from extreme breaking wave investigated more closely with CFD, detailed fatigue analysis at identified hot spots or motion time series for umbilical cable design).

In the **detailed design phase**, the substructure and mooring system are designed up to the level that a certification can be performed and workshop drawings for manufacturing can be produced. There are limitations which from an industrial perspective make the application difficult in the later design stages, i.e. advanced Concept, Basic/FEED and Detailed Design. The main reasons for the challenge in applying the simplified tools are:

- For certification, all recognized standards and classification societies require a simulation and analysis of the full set of design load cases with state-of-the-art software. In this respect, simplified tools are formally not accepted.
- For the wind turbine, once projects enter more detailed loads analyses, detailed loads on RNA components and the tower are required to check if the loads are within the component load envelopes. This level of detail can only be provided by state-of-the-art tools.
- For the substructure hull, an important requirement is to obtain the actual stresses in the steel or concrete structure, down to the detailed stresses in local welds, stiffeners, bulkheads and other structural details. For this level of detail, even current state-of-the-art models are not very well suited and typically a global-local approach is taken, where loads obtained from a global model are transferred onto a more detailed local model, e.g. by means of transfer functions and super-elements (also called influence matrices). Figure 7.2 shows an approach by Ramboll for obtaining detailed stresses within a floater from global coupled simulations. Although the input to this analysis will always be taken from a state-of-the-art model, improved derivation of detailed loads from both the state-of-the-art model and a simplified model may be possible.
- The detailed design of secondary structures and the outfitting, e.g. boat landing, internal ladders, walkways etc. are also part of the detailed design and cannot be designed based on simplified models.
- The mooring system: while the general target stiffnesses can be optimized with QuLAF-like tools, the detailed design requires a more complex analysis, accounting for soil interaction of anchor and mooring line, a detailed design of shackles, top- and bottom-connectors, possible clump weights and buoyancy modules and a detailed non-linear calculations of the design tensions with the mooring lines. This level of detail requires specialized software tools, often then also applied in a global-local approach, where the detailed mooring design is performed with other tools using interface loads and motions from global simulations.

On final comment regarding the optimization with tools such as QuLAF from an industrial viewpoint is related to the tendency to overoptimize designs with respect to the pre-defined cost target functions, which are often primarily weight based. As approximately 70% of the manufacturing cost is governed by early design decisions, it shall be highlighted that in an optimization scheme using simplified tools, much care needs to be taken to define cost functions and also assess the resulting optimal designs from a more holistic viewpoint. This assessment shall then include consideration of manufacturing and logistics constraints, but also possibly aspects of mass production. In a simple case this may e.g. be draft restrictions due to port selection, or main dimension restriction due to storage and fabrication limits in the assembly facility. Also, it may be using standard diameters for certain elements, avoiding complex hull shapes, etc.

Installation aspects for the mooring system are also relevant to consider in this context, e.g. regarding the optimized chain sizes and design tensions, which may make a formally within the optimizer parameter space optimal design in practice rather sub-optimal. For example, for chains above approximately 150 mm size, availability of suitable anchor handling vessels becomes limited and costs highly increase.

Nevertheless, tools such as the herein presented QuLAF, are valuable for industry to become commercially available solutions, particularly to refine the early conceptual design phases. Also the presented statistical methods on critical load case and environmental condition selection are very valuable to limit the considered DLCs in early phases, but also to limit the final design load cases table set, where any omission of certain combinations (e.g. wind wave misalignments) needs to be properly justified.

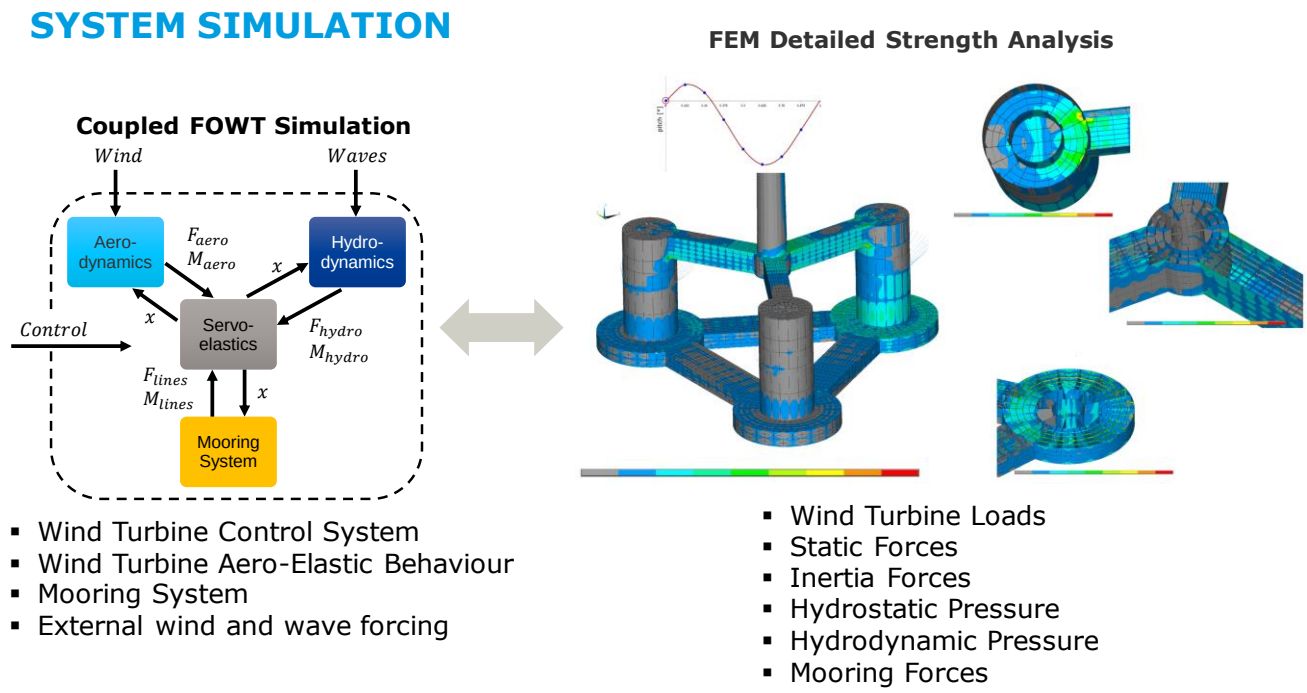

Figure 7.2: System simulation in detailed design stage

8 Conclusion and recommended practices

The purpose of the present deliverable was to answer two questions, namely

- How accurate results can you obtain from simplified models for different load cases?
- In what load cases is it sufficient to apply the simplified models?

Based on a selected subset of critical load cases, this has been investigated through comparison of the simplified model QuLAF and the state-of-the-art model FAST for the OO-Star Wind Floater Semi 10MW floater and the DTU 10MW reference wind turbine. The model accuracy was assessed both in terms of an FLS analysis and a ULS analysis.

The FLS analysis showed that the simplified model was very good at estimating the damage-equivalent bending moment at the tower base, but it had problems with the nacelle acceleration. The high under-prediction in the nacelle acceleration is likely due to the tower being too damped.

The same picture of the nacelle acceleration being too under-predicted in the simplified model was also present in the ULS analysis. The largest tower base bending moments were generally over-predicted, but it was observed that stronger wind would lead to an over-prediction whereas stronger waves would lead to an under-prediction. However, the largest load was obtained at 10.3 m/s in DLC1.6 and here there was a perfect match between the two models. Regarding the platform motions, the largest surge

responses were achieved in DLC1.3 and DLC1.6 with a 3% over-prediction and 11% under-prediction, respectively. The largest heave motions were generally very well matched by the two models and achieves highest values in the ESS (Extreme Sea State) cases. Lastly the ultimate pitch responses were obtained in DLC1.3 and DLC1.6 both at rated conditions and within 4% deviation.

The simplifications in QuLAF lead to model limitations. Most notably the model is restricted to planar motion in aligned wind-wave conditions. Further, three limitations have been identified from the results:

A. An under-prediction of the wave excitation force at large sea states due to the omission of viscous drag forcing. This leads to under-prediction of surge and pitch for strong sea states
B. An under-prediction of the wind-induced response around rated wind speed, where the controller in the full FAST model switches between the partial-load (torque control; fixed blade pitch) and full-load (varying blade pitch; fixed target shaft speed). While the same controller is applied in the decay test, the switching behaviour may not behave similarly.
C. An over-predicted damping for the tower mode motion (at 0.682 Hz). This leads to under-prediction of the nacelle acceleration. Initial results indicate that the damping decreases with frequency. Since the damping of the decay test is based on a clamped tower with rigid blades, the natural frequency of this is (0.51 Hz) lower and thus leads to a larger damping than at the coupled tower frequency. In comparison the full FAST model has a coupled tower frequency of 0.746 Hz when moored and with flexible blades.

Despite these limitations, QuLAF has been found to be a quite accurate load and response prediction tool for aligned wind-wave load cases, especially for tower bending moments, heave and pitch motions. The model can therefore be used as a tool to explore the design space in the preliminary design stages of a floating platform for offshore wind. The model can quickly give an estimate of the main natural frequencies, response and loads for a wide range of environmental conditions, which makes it useful for optimization loops. A full aero-hydro-servo-elastic model is still necessary to assess the performance in a wider range of environmental conditions, including nonlinearities, fault conditions and real-time control.

QuLAF can thus be applied in the pre-design step, where many designs are evaluated and where early decisions on feasibility and are taken. Often these are based on relative load levels and a lower level of accuracy can thus be acceptable. The present study has shown promising results for the co-directional wind-wave restricted versions of DLC 1.2, 1.3, 1.6, 2.1 and 6.1. From the analysis within LIFES50+, these cases are among the design driving load cases for the OO-Star Wind Floater Semi 10MW floating wind turbine configuration. It is stressed that after a concept design has been found, the detailed design verification must be carried out through a full design load basis evaluation with a state-of-the-art model, following established design codes.

9 References

[1] A. Pegalajar-Jurado, H. Bredmose, M. Borg, J. G. Straume, T. Landbø, H. S. Andersen, W. Yu, K. Müller and F. Lemmer, "State-of-the-art model for the LIFES50+ OO-Star Wind Floater Semi 10MW floating wind turbine," *Journal of Physics: Conference Series,* 2018.

[2] A. Pegalajar-Jurado and M. a. B. H. Borg, "An efficient frequency-domain model for quick load analysis of floating offshore wind turbines," *Wind Energy Science Discuss,* vol. In review, 2018.

[3] A. Pegalajar-Jurado, F. Madsen and M. a. B. H. Borg, "D4.5 State-of-the-art models for the two public 10MW concepts. Deliverable of the LIFES50+ project," DTU Wind Energy, 2018.

[4] F. Lemmer, K. Müller, A. Pegalajar-Jurado and M. a. B. H. Borg, "D4.1 Simplified numerical models for up-scaled design.," DTU , 2016.

[5] M. Borg, A. Pegalajar-Jurado, H. Sarlak, F. Madsen, H. Bredmose and F. a. B. F. Lemmer, "D4.7 Models for advanced load effects and loads at component level. Deliverable of the LIFES50+ project.," 2018.

[6] K. Müller, Faerron-Guzmán and M. a. M. A. Borg, "D7.7 Identification of critical environmental conditons and design load cases. Deliverable of the LIFES50+ project".

[7] W. Yu, K. Müller and F. Lemmer, "LIFES50+ D4.2: Public definition of the two LIFES50+ 10MW floater concepts," University of Stuttgart, 2018.

[8] C. Bak, F. Zahle, R. Bitsche, T. Kim, A. Yde, L. C. Henriksen, A. Natarajan and M. H. Hansen, "Description of the DTU 10MW Reference Wind Turbine," DTU Wind Energy Report I-0092, 2013.

[9] M. Borg, M. Mirzaei and H. Bredmose, "LIFES50+ D1.2: Wind turbine models for the design," Technical University of Denmark, 2015.

[10] M. H. Hansen and L. C. Henriksen, "Basic DTU Wind Energy controller," DTU Wind Energy Report E-0028, 2013.

[11] M. H. Hansen, A. Hansen, T. J. Larsen, S. Øye, P. Sørensen and P. Fuglsang, "Control design for a pitch-regulated, variable-speed wind turbine," Risø National Laboratory Technical Report Risø-R-1500(EN), 2005.

[12] C. H. Lee and J. N. Newman, "WAMIT homepage," WAMIT, Inc., [Online]. Available: http://www.wamit.com/index.htm. [Accessed 4 October 2017].

[13] W. E. Cummins, "The impulse response function and ship motions," *Schiffstechnik,* vol. 9, pp. 101-109, 1962.

[14] M. Hall, "MoorDyn User's Guide," Department of Mechanical Engineering, University of Maine, 2015.

[15] S. Schløer, L. Castillo, M. Fejerskov and E. a. B. H. Stroescu, “A model for quick load analysis for monopile-type offshore wind turbine structures,” *Wind Energy Science,* vol. 3, pp. 57-73, 2018.

[16] A. Krieger, G. K. V. Ramachandran, L. Vita, P. Gómez Alonso, G. González Almería, J. Berque and G. Aguirre, “LIFES50+ D7.2: Design basis,” DNV-GL, 2015.

[17] K. Müller, F. Lemmer, F. Borisade, M. Kretschmer, N.-D. Nguyen and L. Vita, “State-of-the-Art FOWT Design Practice and Guidelines,” *LIFES50+ Deliverable 7.4,* 03 2016.

[18] International Electrotechnical Commission , "Wind Turbines - Part 3: Design Requirements for Offshore Wind Turbines," *61400-03,* 2009.

[19] Det Norske Veritas AS, "Design of Floating Wind Turbine Structures," *DNV-OS-J103,* 2013.

[20] International Electrical Commision, *IEC 61400 - Part 3: Design requirements for offshore wind turbines,* International Electrical Commision, 2009.